M Sc. in Mechanical Engineering Thesis

# Parametric Analysis of Thermal performance of Earth-To-Air-Tunnel-Heat Exchanger (EATHE)


Submitted By

**Masud Rana**

161011007

Supervised By

**Arafat Ahmed Bhuiyan, PhD**


**A Thesis submitted in partial fulfillment of the requirement for the degree of Master of Science in Mechanical Engineering**



**Department of Mechanical and Production Engineering (MPE)**

**Islamic University of Technology (IUT)**


**August, 2022**

# Candidate's Declaration

This is to certify that the work presented in this thesis, titled, "Parametric Analysis of Thermal performance of Earth-To-Air-Tunnel-Heat Exchanger (EATHE)", is the outcome of the investigation and research carried out by me under the supervision of Dr. Arafat Ahmed Bhuiyan.

It is also declared that neither this thesis nor any part of it has not been submitted elsewhere for the award of any degree or diploma.

---

Masud Rana

161011007

## RECOMMENDATION OF THE BOARD OF EXAMINERS

The thesis titled ***"Parametric Analysis of Thermal Performance of Earth-to-Air-Tunnel-Heat Exchanger (EATHE)"*** submitted by Masud Rana, Student number: 161011007 has been accepted as satisfactory in partial fulfillment of the requirements for the degree of M Sc. in Mechanical Engineering on 26th August, 2022.

## BOARD OF EXAMINERS

1. ----------
   Dr. Arafat Ahmed Bhuiyan — Chairman (Supervisor)
   Associate Professor
   MPE Dept., IUT, Board Bazar, Gazipur-1704, Bangladesh.

2. ----------
   Dr. Md. Anayet Ullah Patwari — Member (Ex-Officio)
   Professor and Head
   MPE Dept., IUT, Board Bazar, Gazipur-1704, Bangladesh.

3. ----------
   Dr. Md. Hamidur Rahman — Member (Internal)
   Professor
   MPE Dept., IUT, Board Bazar, Gazipur-1704, Bangladesh.

4. ----------
   Dr. A K M Sadrul Islam — Member (External)
   Managing Director
   The IBN SINA Pharmaceuticals Industry Ltd, Dhaka.
   &
   Former Professor and Head
   MCE Dept., IUT, Board Bazar, Gazipur-1704, Bangladesh.

## ACKNOWLEDGEMENTS

First and foremost, all praise is paid to the Almighty Allah for giving me the knowledge and the ability to think and helping me finish my thesis with His inexhaustible kindness.

I thank Dr. Arafat Ahmed Bhuiyan for his continuous guidance and valuable advice on my research and thesis work. His constant assistance, inspiration, guidance, and valuable suggestions throughout the research work have made this thesis successful. Furthermore, his commitment to excellence has motivated me, now and in my future career.

Deepest gratitude to Md. Emran Hossain Moin and Md. Kabbir Hoissain, BSc students in the Department of Mechanical and Production Engineering (MPE), Islamic University of Technology (IUT), for their help throughout this work.

Finally, I appreciate the continued support from staff members of the Departments of Mechanical and Production Engineering and my fellow graduate students.

Masud Rana

## Abstract

The Earth-to-Air-Tunnel-Heat Exchanger (EATHE) is one of several ambient air conditioning systems with minimum cost. Several factors and conditions will enhance the performance of the installed EATHE in room air conditioning system. In this numerical study, the influence of ground soil considering its properties, such as soil thermal conductivity, room air conditions such as air velocity, and construction of the system such as pipe thickness and length on the EATHE is investigated. Later, different arrays of fins are introduced to enhance the system's performance further. Finally, the model has been validated by comparing the outlet temperature of the system with the experimental results conducted by other researchers.

The current study analyzes the thermal performance based on three miscellaneous soil samples, each with thermal conductivity of 0.65 $Wm^{-1}K^{-1}$, 1.25 $Wm^{-1}K^{-1,}$ and 3.5 $Wm^{-1}K^{-1}$, respectively. The effect of the thermal conductivity of soil due to geographic locations on the thermal performance of the EATHE system is significant. The thermal efficiency of the EATHE has been determined by the reduction in air temperature caused by transient heat transfer between the air and soil around the pipe. The effect of the soil layer is negligible after a critical thickness. The critical thickness is considered to be ten times the pipe diameter. The maximum temperature reduction is 18.9 K for 3.5 $Wm^{-1}K^{-1}$ thermal conductivity at a specific air velocity of 3 $ms^{-1}$. A new model for a 10 m long pipe with various fin/fins arrangements has been created. The effects of fins were analyzed by placing a single fin of 10 mm at 0.5 m from the inlet and getting an outlet temperature of 306.7 K. The drop in temperature evolves with four fins at 0.5 m, 1 m, 1.5 m, and 2 m, and the found minimum temperature is 306.1 K, which is 19.4% more improved than a straight pipe. If fins are spaced 1m apart, the temperature drop increases by 5.6%. The arrangement with four fins at 2 m spacing gives an outlet temperature of 305.3 K, which is 7% better than a single fin. A new arrangement of fins has been used to observe their effect on the

heat dissipation rate. In this arrangement, fins of 10 mm in thickness and different heights have been used in diverging-converging patterns to restrict the flow of air and thus supply cooled air at the outlet. The investigation with two blocks improves outlet temperature by 5.88% over the analysis with one block. The value progresses to 10.53% for three blocks and 14.52% for four blocks relative to the temperature drop of one block. Overall, this study will provide a comprehensive understanding of the design parameters and associated conditions, leading to enhanced performance of the EATHE.

# List of Symbols and Abbreviations

**Symbols**

| | |
|---|---|
| $C_p$ | Local pressure coefficient |
| $C_p$ | Average pressure coefficient |
| $C_\varepsilon$ | k-ε turbulence model coefficient |
| $C_\mu$ | k-ε turbulence model viscosity constant |
| $C_\omega$ | k-ε turbulence model constant |
| c | Specific heat at constant pressure |
| D | Tube diameter |
| $D_h$ | Hydraulic diameter |
| f | Friction factor |
| $f_\eta$ | RNG k-ε turbulence model coefficient |
| $f_\mu$ | Zero equation turbulence model constant |
| h | Average heat transfer coefficient |
| $h_e$ | Specific enthalpy |
| j/f | Efficiency index |
| K | Kelvin |
| k | Turbulence kinetic energy |
| L | Pipe Length |
| m | Mass flow rate |
| $N_u$ | Local Nusselt Number |
| $N_u$ | Average Nusselt Number |
| $P_r$ | Prandtl Numer |
| Q | Average heat flux |
| Q'' | Heat flux |
| $R_e$ | Reynolds number based on hydraulic diameter, Dh |
| $S_E$ | Energy source |
| $S_M$ | Momentum source |
| $S_t$ | Stanton Number |
| T | Temperature |
| $T_b$ | Bulk mean temperature |

| | |
|---|---|
| $T_{in}$ | Inlet temperature |
| $T_w$ | Wall temperature |
| U | Dimensionless velocity vector |
| u | Velocity components in x- coordinate direction |
| v | Velocity components in y- coordinate direction |
| w | Velocity components in z- coordinate direction |
| $\alpha$ | k-ε turbulence model constant |
| $\beta$ | k-ε turbulence model constant |
| $\varepsilon$ | Turbulence dissipation rate |
| $\nu$ | Kinematic viscosity |
| $\lambda$ | Thermal conductivity |
| $\mu$ | Dynamic viscosity |
| $\zeta$ | Bulk viscosity |
| $\rho$ | Fluid density |
| $\sigma$ | Stress tensor including pressure |
| $\sigma_k$ | k-ε turbulence model coefficient |
| $\sigma_\varepsilon$ | k-ε turbulence model coefficient |
| $\sigma_\omega$ | k-ω turbulence model coefficient |
| $\sigma_\Phi$ | Stress tensor for an additional variable |
| $\tau$ | Shear stress |
| $\tau_\omega$ | Wall shear stress |
| $\tau$ | Reynolds Shear stress |

**Abbreviations**

| | |
|---|---|
| CFD | Computational fluid dynamics |
| EAHEs | Earth Air Heat Exchanger |
| EATHE | Earth to Air Tunnel Heat Exchanger |
| FVM | Finite Volume Method |
| GSHP | Ground Source Heat Pump |
| LMTD | Log mean temperature difference |
| PVC | Poly Vinyl Chloride |

# Contents

## List of Figures

## List of Tables

# 1. Chapter: Introduction

## 1.1. EATHE system

With each passing day, there is increasing interest in installing geothermal energy-based heating and cooling systems for buildings. The soil attenuates temperature changes at the ground surface because of its considerable thermal inertia. In recent year's use of geothermal energy are increased rapidly. It can consider suitable energy source is geothermal energy. Using geothermal energy for services like reducing a building's heating and cooling demands is becoming more widespread daily. Given the global energy crisis and the importance of energy to our society's survival, conserving energy and improving overall energy efficiency is crucial and necessary. Active heating and cooling systems are not more efficient than passive heating and cooling systems. Passive heating and cooling systems can consume little or no energy. The Earth to Air Tunnel Heat Exchanger (EATHE) is one of several ambient air conditioning systems[1]. It has a distinct benefit over most passive systems in that it can produce warmth and cooling in the winter and summer.

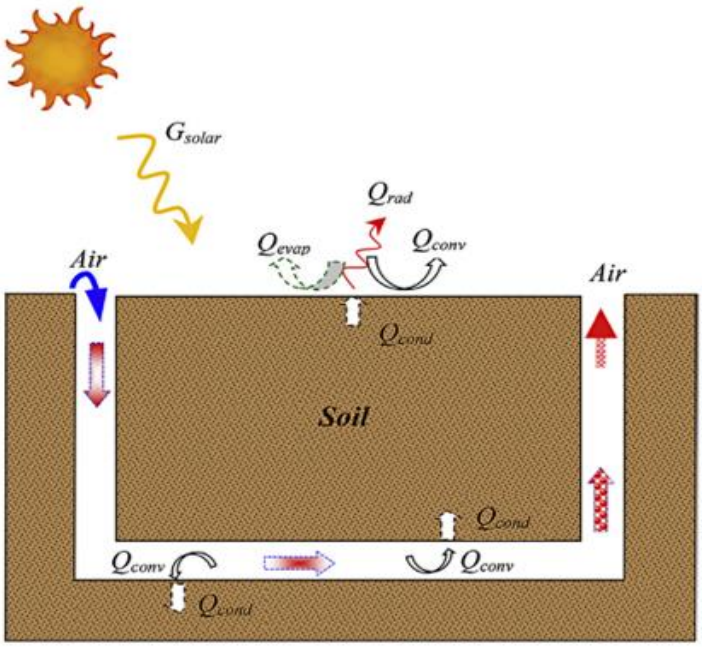


**Figure 1**: A Simple Model of EATHE [1]

The Earth is a vast heat sink and storage medium utilized daily or during seasons. Because of its enormous heat capacity and insulating capabilities, the ground has numerous advantages. Similarly, the Earth's heat capacity is such that daily surface temperature changes do not reach depths greater than 0.5 m. For seasonal variations, temperature differences do not reach depths greater than 3 m. Below this depth temperature of the earth remains unchanged, and the yearly mean of the soil air temperature at the surface is commonly used to calculate this temperature [2]. Hence, the outside air temperature is always lower than the ground temperature at a sufficient depth. But in the summer, the ground temperature is lower than the surface. The potentiality of the earth's thermal can be transacted using EATHE, as shown in **Figure 1**. This system has been utilized to reduce the usage of primary energy resources in space by acting as a passive heating/cooling approach. It is made up of a long subterranean metal or plastic pipe that is used to pull air. During the periods of heating, fluid travels through the pipe. When air travels on the pipe, they release some heat to the ambient soil or receives some heat from the ambient soil. This air entering the house is considered conditioned air. In cold countries, the Earth Air Tunnel Heat Exchanger, also known as an earth tube heat exchanger, has much potential for space heating. An EATHE system consists of one or more pipe/pipes arranged in a specific pattern and set to a particular depth in the floor. A blower is used to blow air from the room through the pipes. The air blasted through the pipes swaps heat with the nearby earth layers before being given to the building's inhabited space.

### 1.2. Background

Except for a few traditional energy inputs, these passive alternatives rely on natural energy sources (usually to operate a small fan for air). Through various approaches, geothermal power has long been acknowledged as one of the most abundant sources for heating and cooling buildings. It mainly started three decades after 1973's oil crisis [3, 4]. Mainly, the many

techniques to use geothermal energy that has been developed thus far are as follows: (i) Earth-air heat exchanger system (EAHEs) or Earth air tunnel system (EATs) [5-7]; (ii) direct integration of the building envelope [8, 9]; and finally (iii) Ground source heat pumps (GSHP) [10, 11]. These are used to harness the earth's thermal energy for air conditioning. In a standard Earth air tunnel heat exchanger, the air is pushed to exchange heat with the soil through tunnels/pipes buried in the ground, and the air is thus heated/cooled based on the temperature difference between air and soil. This heated/cooled air is utilized directly or indirectly in indoor environments to provide thermal comfort. In the second alternative, the buildings themselves exchange heat with the soil through their whole or partly subsurface construction. [12, 13]. However, this approach necessitates extensive soil excavation, which raises expenses considerably. In a third method, the soil heat exchanger is utilized in conjunction with a closed circuit GSHP system of long tubes buried in the ground (typically PVC). The extracted soil heat is used to heat/cool indoor spaces and in domestic applications [14-17], to melt snow or ice accumulated on the pavement or bridge surfaces in winter [18, 19]. The solutions above have proven their worth by lowering condensation temperatures throughout the summer and increasing evaporation temperatures during the winter. [20]. The Earth Air Tunnel (EATHE) Heat Exchangers are simple in design and substantially less expensive because they use air as a working fluid and require just a minimal amount of electric power to operate. The ground temperature are fluctuates with depth and remains nearly unchangeable at 4 m or higher [21]. This constant temperature is different from the average seasonal temperature in the summer and higher than the average seasonal temperature in the winter [22]. EATHEs use thus the difference between the subsoil and ambient air temperature to heat the air in winter and cool the air in the summer. Many researchers have reported progress in the different aspects of EATHEs, while some recommended it as a feasible and effective alternative source of passive energy for space heating/cooling [12, 23, 24]. Many scientists have carried out extensive research on different aspects of EATHEs. Recently, Leyla

Ozgener [25], Bisoniya et al. [26], Peretti et al. [27], and Kaushal [28] have published thorough reviews on EATHEs. An important factor to consider while studying EATHEs is the soil properties. Soil's performance is based on input temperature that varies seasonally and the temperature of the earth, as well as the moisture distribution in the soil [29]. Various statistical characteristics of soil surface temperatures at various depths and analyzed by Jacovides et al. [3]. Puri [30] looked at the diameter of a pipe buried in the ground conveying a hot fluid, as well as the initial soil moisture concentration, temperature, and temperature of the fluid tube contact. Bojic et al. [31] and Krarti et al. [32] analyzed the technological and financial performance of an Earth air tunnel heat exchanger using several mathematical models. A 3-D non-steady state flow model was established by Deglin et al. [33] to explore the effects of different soils and pipes on the performance of the EATHE. Thiers and Peuportier proposed a technical solution to reduce building heating and cooling energy consumption[34]. Other researchers based their experimental studies on the effects of various parameters like material, length, diameter, thickness, number, and spacing of the buried pipes, soil type, depth of the pipes under the soil, inlet air velocity, etc. Bansal et al. [35, 36] found a great resemblance between simulated data with the experimental ones and found that the COP of the EATHE system increases with the increase of velocity. On further research, Bansal et al. [37] stated that higher soil thermal conductivity always results in a better thermal performance of the EATHE. Bansal et al. [38] also studied that the temperature rise of soil layers is greater for the first length of the pipe than for the subsequent length, according to the thermal influence zone. The performance of a solar PV assisted EATHE was investigated by Yildiz et al.[39] by exergetic analysis based on parameters like climatic condition, sand condition etc. Misra et al. [40-42] mentioned in their study that, derating factor (ratio of the deterioration in thermal performance of EATHE under transient condition to the thermal performance under steady state condition) can be as high as 64% and thus put emphasis on the fact that, while designing an EATHE, derating factor must be taken into

consideration. They also found that derating factor is a function of soil thermal conductivity, duration of cont. operation and pipe length. The deteriorating performance of EATHEs with the increased pipe diameter and increased flow velocity was shown by Misra et al. [42]. Li et al. [43] coupled an earth to air heat exchanger with a solar chimney and found promising performance. Longer pipes and higher depths of burial for obtaining better performance from the EATHEs were recommended by Wu et al. [22]. Mathur et al. [44] concluded that the deteriorating performance of EATHEs due to continuous operations could be compensated by increasing the pipe length. In a different study, Mathur et al. [45] compared the performance between EATHEs having straight and spiral pipe's and stated that spiral pipe's performance is comparable to that of the straight ones while having a lower aspect ratio. Few researchers [46-49] investigated the arrangements of multiple buried pipes. Misra et al. [40] concluded that the thermal influence zone has a conical shape (narrower towards the end) and thus suggested that the spacing between the buried pipes should be gradually decreased along the pipe length. Kabashnikov et al. [48] developed a mathematical model in the form of Fourier integral and found that the efficiency of the EATH decreases with the decrease in the spacing between the buried pipes. Sodha et al. [49] analyzed the performances of the parallel pipes with respect to each other. A few other [50-52] researchers discussed an alternative to the continuous operation; intermittent operation of the EATHE system. Mathur et al. [51] suggested running the EATHE in winter days/night mode to get a better performance in the following summer as it will reduce the soil saturation. It was recommended by Mathur et al. [50] that, during the OFF phase, the soil temperature and cooling capacity can recover in the intermittent mode. It was shown by Mathur et al. [52] that, intermittent operations (60 min ON and 20 min OFF) increases the heat transfer rate by 1.81% in terms of the outlet temperature.

### 1.3. Scope of the Study

Investigation into the relationship of EATHE pipe configurations, ambient circumstances, and soil qualities is recommended to optimize thermal performance. The EATHE's thermal efficiency will be investigated by how much the air temperature drops when heat moves from the air to the soil around the pipe. The effect of the thermal conductivity of soil due to geographic location on the thermal performance of the EATHE system is significant. However, the majority of the work has been done in frigid climates. Because of this, it is essential to build an accurate EATHE model to determine how much the EATHE's performance has dropped due to the system's constant use in hot summer weather. Additionally, it is necessary to investigate how to enhance pipe design to increase heat transfer efficiency.

### 1.4. Objectives with Specific Aims

The main objectives of the present study are to investigate the parametric effects on the performance of earth to air tunnel heat exchangers. The following is a detailed outline of the study's significant purposes at each stage.

1. Develop an accurate Earth Air Tunnel Heat Exchanger (EATHE) model and to validate the model by comparing it with the experimental result.
2. Study the effect of variation of pipe length of operation on its thermal performance.
3. Study the effects of variation of soil properties and soil thickness under room conditions.
4. Study the effect of fin arrangements and fin blocks under different flow conditions.

### 1.5. Possible Outcomes

1. Impact of the thermal conductivity and soil thickness of the ground around the EATHE pipe will be determined.

2. Impact of multiple fin layouts and blocks of the fin in the newly designed PVC will be investigated.
3. Impact of pipe length and room conditions on the heat transfer performance will be determined.
4. Selection of optimum conditions for enhanced heat transfer performance will be predicted.

### 1.6. Structure of the Thesis

This first chapter of the thesis will discuss the basic understanding of the EATHE system, its function, advantages, disadvantages, recent and previous work, and passive heating and cooling system. In the current year's use of geothermal energy are increased rapidly; EATHE is a system based on geothermal energy. This system has been utilized to reduce the usage of primary energy resources in space by acting as a passive heating/cooling approach. Since it can generate heating and cooling in the winter and summer, it has a clear advantage over most passive systems. Furthermore, this system operates without additional hardware, such as an air conditioning unit or an air compression device. This chapter also discusses the thesis's main objective and possible outcomes.

The second chapter discusses the configuration of the EATHE system. One or more pipe/pipes are arranged in a specific pattern and set to a particular depth to draw air through it. In this chapter also discuss the impact of the soil thermal conductivity. The soil's thermal conductivity significantly impacts the thermal efficiency of the EATHE system as a result of the system's geographic location. The effect of the pipe's length, fins, and thickness are all glamorous issues in this chapter.

The third chapter discusses all of the numerical equations used to support this thesis are described here. Heat transmission, divided into thermal convection and thermal conduction, happens in the EATHE system. Thermal convection occurs between the inner pipe surface and the air traveling through it, and thermal conduction occurs between the outer pipe surface and the

surrounding earth. This system is analyzed by the Finite Volume Method using meshing for Finite Control Volumes. Each control volume's governing equations are integrated, resulting in discrete conservation. All those equations and constants are described in this chapter.

The fourth Chapter discusses the numerical model of the EATHE system. All the condition of the numerical approach is described in this section. This chapter covers a wide range of topics, including inlet conditions; soil far boundary, inlet, exit face, interface condition, and outlet condition. In addition, the physical and thermal characteristics of the various simulated materials and all the geometric parameters of EATHE are included in this chapter. The thermal performance of an EATHE system is evaluated with a CFD model. It can predict fluid flow, fluidity, and compressibility events in various conditions, including compressible, incompressible, laminar, and turbulent cases.

The results and conclusions are then addressed, including the current investigation of the effect of thermal conductivity of soil, the thermal performance based on three different soil samples, each having a different thermal conductivity of 0.65 $Wm^{-1}K^{-1}$, 1.25 $Wm^{-1}K^{-1,}$ and 3.5 $Wm^{-1}K^{-1}$. The effect on thermal performance is investigated for different types of air velocities entering the EATHE ranging from 3 $ms^{-1}$ to 6 $ms^{-1}$ to analyze the thickness of the PVC pipe.

# 2. Chapter: Problem Formulation

## 2.1. Configurations of The Earth To Air Tunnel Heat Exchangers

An EATHE uses a lengthy subsurface metal or plastic (PVC) conduit to draw air through it. This system has been utilized to reduce the usage of primary energy resources in space by acting as a passive heating/cooling approach. It is made up of a long subterranean metal or plastic pipe used to pull air. Fluid travels through the pipe during heating. When air moves through the pipe, it either gives some heat to the soil around it or takes some heat from it. The air that comes into the house is called "conditioned air."

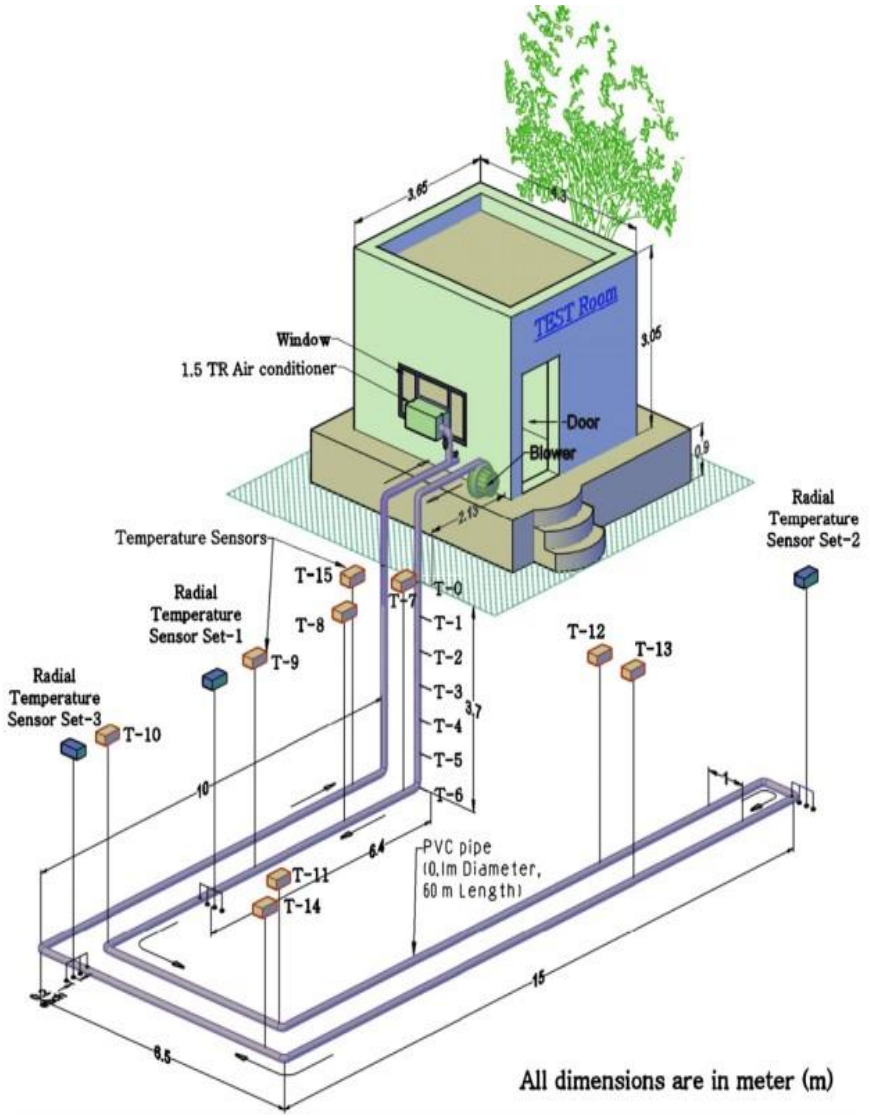


**Figure 2**: Schematic diagram of room integrated EATHE system [37]

The system comprises one or more pipe/pipes arranged in a specific pattern and set to a particular depth in the floor, together with a blower that blows air through the pipe (s). The air blasted through the pipes interchange heat with the nearby earth layers before being given to the building's inhabited space. The fluctuation of underground soil's temperature depends on its depth, but after a certain distance becomes nearly constant. It was investigated by Mathur et al. [50] that, after 4 m or higher, the soil temperature becomes nearly constant. This constant temperature has the distinct attribute of being below average summer season temperature and above average winter season temperature. EATHEs use thus the variety between the underground soil and circumfluent air temperature to heat the air in the wintertime and to cool the air in the summertime.

## 2.2. Impact of the soil thermal conductivity on heat exchangers

The soil properties are a significant consideration while analyzing EATHEs. The performance of soil, temperature, and moisture distribution inside the earth is determined by the input temperature in different seasons [29]. Various statistical characteristics of soil surface temperatures at various depths were analyzed by Jacovides et al.[3]. Puri [30] talked about a pipe that was put into the ground and carried hot fluid. He focused on the causes, such as the diameter of the pipe, the initial soil moisture and concentration, and the temperature and heat of the inner and outer surfaces of the fluid tube. The heat conductivity of soil is heavily influenced by its saturation and dry density. The dry density is the number of soil particles per unit volume, while saturation is the amount of moisture in the soil. The soil's thermal conductivity goes up when its density goes up, either when it's wet or when it's dry. Soil thermal conductivity is also affected by mineral content, weather, soil texture, and time. .

## 2.3. Impact of the pipe length on heat exchangers

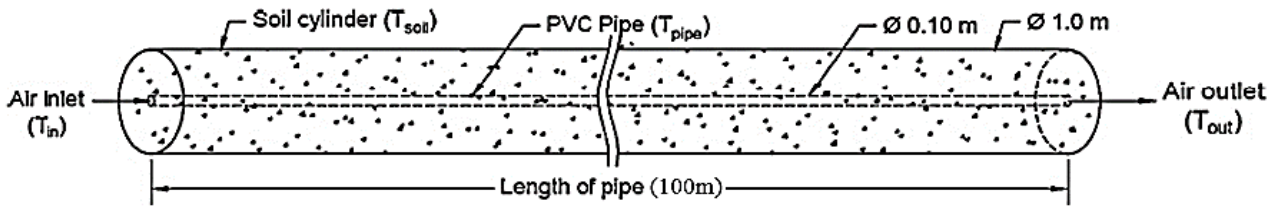


(a)

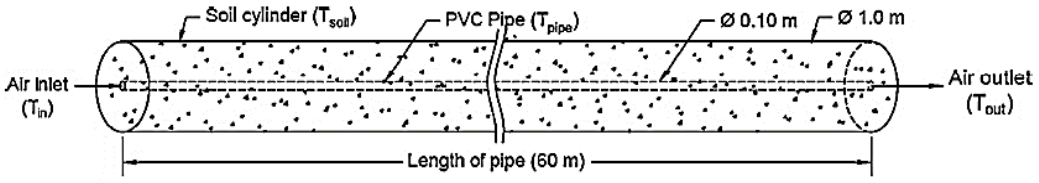


(b)

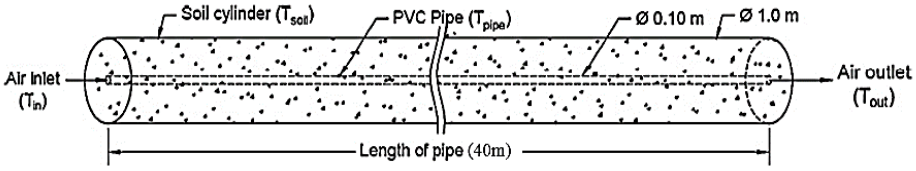


(c)

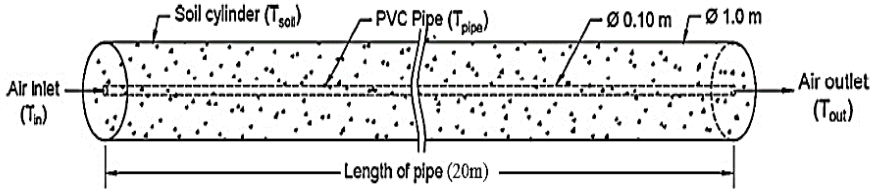


(d)

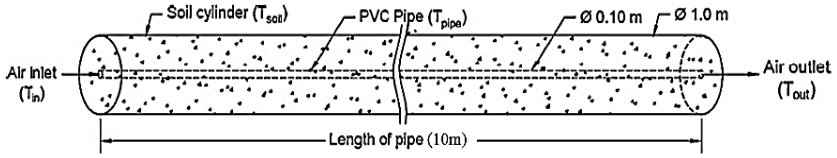


(e)

**Figure 3**: Schematic diagram of (a) 100 m long pipe (b) 60 m long pipe (c) 40 m long pipe (d) 20 m long pipe (e) 10m long pipe.

When developing a maximum horizontal heat exchanger on underground soil, an essential factor is the soil's thermal conductivity needs to be considered. Because of its particle structure, soil thermal conductivity is significantly affected by its density and water content. Different techniques are used to study the effect of thermal conductivity, soil type, and moisture content on the horizontal ground heat exchanger. Those considerations are taken to develop a horizontal heat exchanger design. **Figure 3** shows that the design pipe length for a horizontal ground heat exchanger can be cut by making the soil more thermally conductive. When the pipe length gets longer, friction pushes against the flow, which makes the pressure go down. The factors of pipe length and fittings increase the "length" input for the equation. Pressure loss and efficiency decrease as flow velocity increases. Based on these models, numerical simulations and special experimental investigations were carried out.

### 2.4. Impact of the fin on pipe length

Fins are the extended surface. Heat transfer is augmented by increasing surface area. The temperature difference between a body and its environment affects the rate of heat loss. The fact that the temperature gradient is slight and the nature of the heat transmission mechanism remains unchanged tempers the law of cooling. This condition is frequently met in thermal conduction since the thermal conductivity of most materials is relatively unaffected by temperature. Plain fins, on the other hand, have a worse heat transfer performance than specifically constructed fin surfaces.

Nevertheless, certain fin types are still extensively utilized when minimal pressure drop qualities are desired. For example, adding a fin to an object height of 20mm and a wide 10mm increases the surface area and creates a maximum temperature drop, as shown in **Figure 4**. Furthermore, the EATHE results are followed by additional heat transfer regions or constrictions where the air

can release heat to the soil nearby. In that case, it can be concluded that the EATHE can be employed to save more energy.

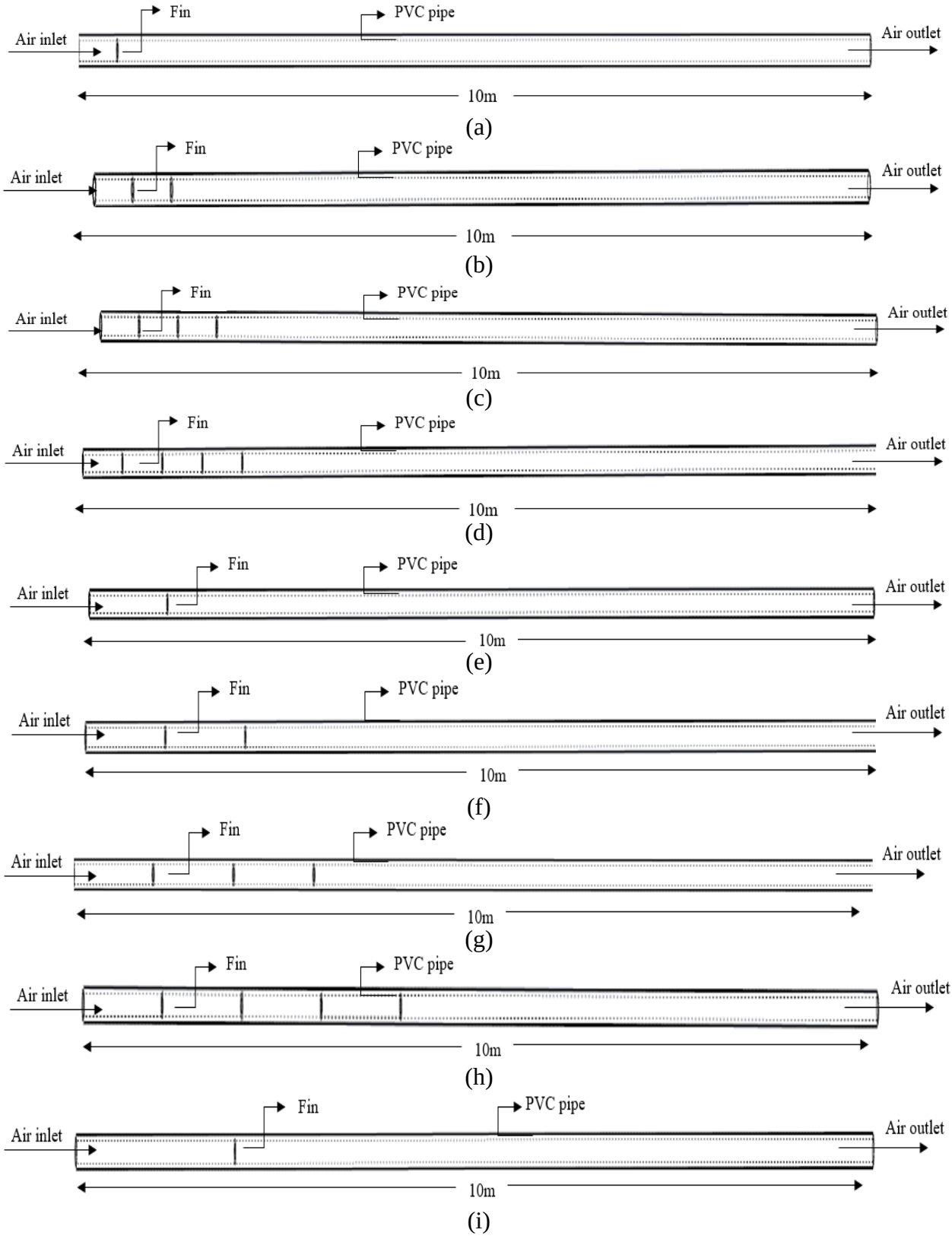

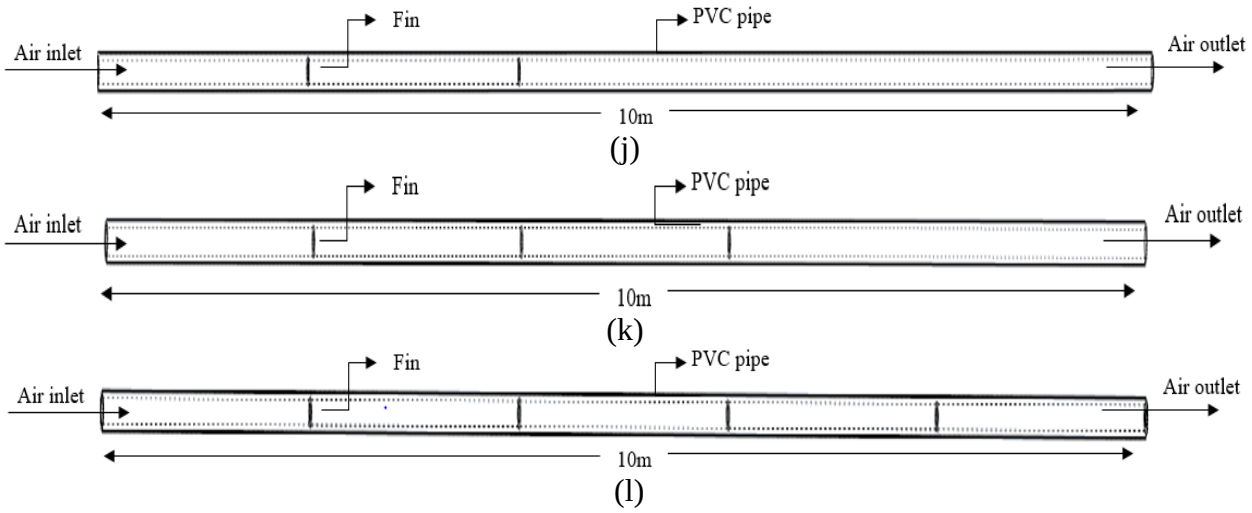


**Figure 4:** The computational domain of 10m long pipe with (a) 1 fin after 0.5m (b) 2 fins after 0.5m (c) 3 fins after 0.5m (d) 4 fins after 0.5m (e) 1 fin after 1m (f) 2 fins after 1m (g) 3 fins after 1m (h) 4 fins after 1m (i) 1 fin after 2m (j) 2 fins after 2m (k) 3 fins after 2m (l) 4 fins after 2m

## 2.5. Impact of the block on pipe length

Replacing the fins of 10mm thickness, a new arrangement of fins has been used to observe their effect on heat dissipation rate. In this arrangement, fins of 10mm thickness and different heights have been used in diverging-converging patterns to restrict airflow and thus supply cooler air at the outlet. **Figure 5** shows the inner cross-section of a single block, and Each block consists of 5 fins of 15mm, 20mm, 25mm, 20mm, and 15mm height placed equidistantly stretching to 2.5m on the air to the boundary wall surface. **Figure 6** shows that when one block is implemented in EATHE system, it takes the first quarter from the inlet.

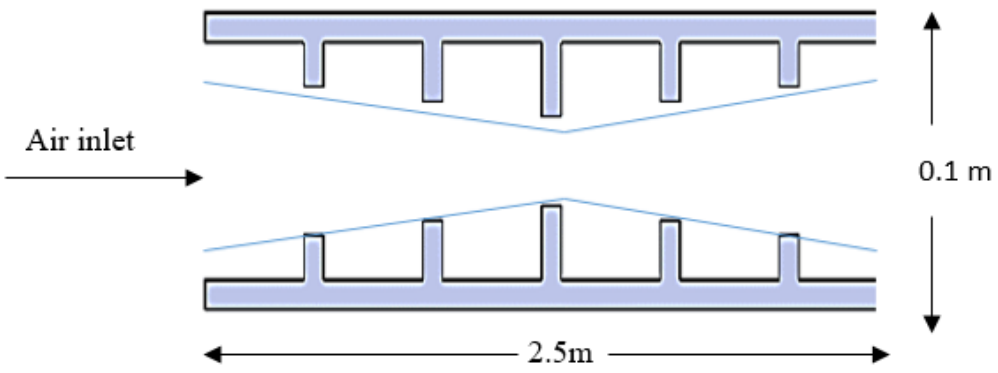


**Figure 5**: 2D view of a single block

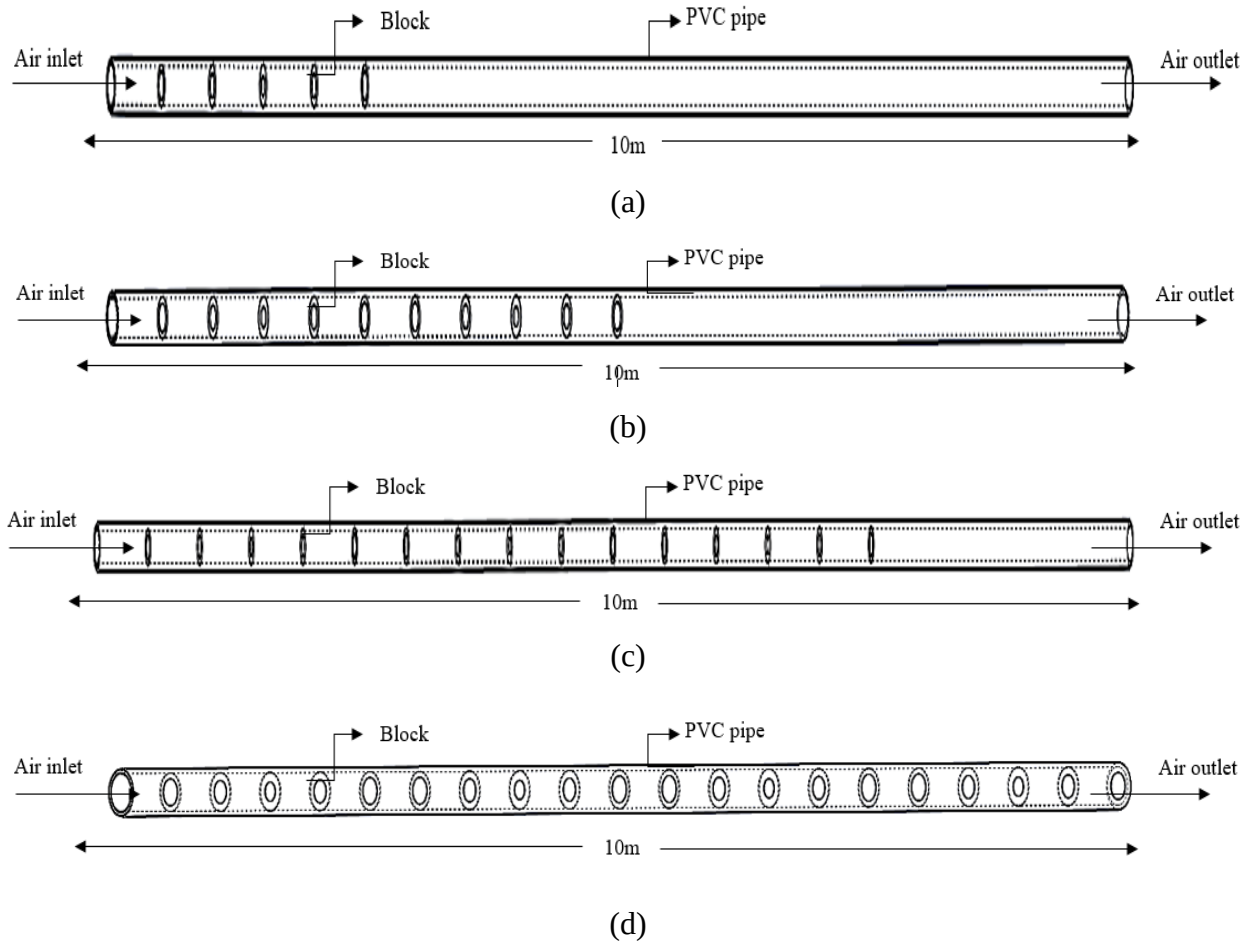


**Figure 6**: Schematic representation of 10m long pipe with (a) single block, (b) two blocks, (c) three blocks (d) four blocks.

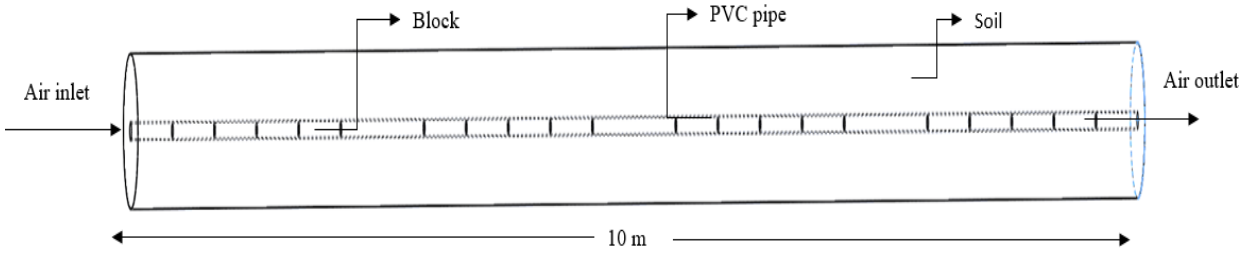


**Figure 7**: 10m long pipe with four blocks and soil layer

# 3. Chapter: Governing Equations

## 3.1. Model description

The air that passes through the pipe either gives off some heat to the surrounding soil or absorbs some heat from the surrounding soil. This physical system's heat transfer is classified into thermal convection and conduction. The process of thermal convection occurs between the air passing through the pipe and the surface of the pipe itself, and the process of heat conduction occurs between the pipe's exterior surface and the soil's environment surrounding the pipe. This research is carried out with the help of ANSYS 19.0, a commercial computational fluid dynamics (CFD) program. The Finite Volume Method (FVM) is used in this code. This method discretizes the spatial domain into finite control volumes using the mesh. Each control volume's governing equations are integrated, resulting in discrete conservation of key variables (mass, momentum, and energy) for each control volume. An algebraic multi-grid approach is employed to speed up the solver's convergence using a set of coarse grid levels to calculate the corrections. The momentum and energy equations are discretized using the second-order upwind approach in all simulations.

The continuity and Navier-Stokes laws for the conservation of mass and momentum define the flow along with the energy equations. The laminar model is sensitive to the amount of mixing, the scalar dissipation, and the passage of time. The following are the fundamental equations used to explain flows in three dimensions. :

The equation of Continuity: $\frac{\partial u}{\partial x}+\frac{\partial v}{\partial y}+\frac{\partial w}{\partial z}=0$ (3.1)

The momentum equation:

Component (X): $u\frac{\partial u}{\partial x}+v\frac{\partial u}{\partial y}+w\frac{\partial u}{\partial z}=-\frac{\partial p}{\partial x}+\frac{1}{Re_H}\left(\frac{\partial^2 u}{\partial x^2}+\frac{\partial^2 u}{\partial y^2}+\frac{\partial^2 u}{\partial z^2}\right)$ (3.2)

Component (Y): $u\frac{\partial v}{\partial x}+v\frac{\partial v}{\partial y}+w\frac{\partial v}{\partial z}=-\frac{\partial p}{\partial y}+\frac{1}{Re_H}\left(\frac{\partial^2 v}{\partial x^2}+\frac{\partial^2 v}{\partial y^2}+\frac{\partial^2 v}{\partial z^2}\right)$ (3.3)

Component (Z): $u\frac{\partial w}{\partial x}+v\frac{\partial w}{\partial y}+w\frac{\partial w}{\partial z}=-\frac{\partial p}{\partial z}+\frac{1}{Re_H}\left(\frac{\partial^2 w}{\partial x^2}+\frac{\partial^2 w}{\partial y^2}+\frac{\partial^2 w}{\partial z^2}\right)$ (3.4)

The Energy Equation (E): $u\frac{\partial \theta}{\partial x}+v\frac{\partial \theta}{\partial y}+w\frac{\partial \theta}{\partial z}=\frac{1}{Re_H Pr}\left(\frac{\partial^2 \theta}{\partial x^2}+\frac{\partial^2 \theta}{\partial y^2}+\frac{\partial^2 \theta}{\partial z^2}\right)$ (3.5)

Here, non-dimensional temperature, $\theta=\frac{(T-T_w)}{(T_{in}-T_w)}$ (3.6)

In this study, k-ε model is considered for turbulence modeling. Turbulence is a series of small-scale changes in flow properties over time. It's a complicated process because it's three-dimensional, unstable, chaotic and can change the flow's characteristics significantly. Turbulence occurs when the fluid's inertia forces become larger compared to viscous forces, and high Reynolds numbers characterize it. A lot of CFD research has developed methods that employ turbulence models to forecast the consequences of turbulence. Turbulence models were explicitly created to account for the effects of turbulence without resorting to an impractically thin mesh or direct numerical simulation. The kinetic energy of turbulence, denoted by the symbol "k" has the dimensions ($L^2T^{-2}$) and the unit "$m^2/s^2$," and it indicates the velocity profile on the variance of the fluctuations. The turbulent eddy dissipation parameter is "ε'" with dimensions of ($L^2T^{-3}$) and a unit of $m^2/s^3$. In the k-ε model, two more variables are included in the equations system. The following are the governing equations based on the study's assumptions:

The continuity equation: $\frac{\partial u}{\partial x}+\frac{\partial v}{\partial y}+\frac{\partial w}{\partial z}=0$ (3.7)

The momentum equation:

Component (X):

$\frac{\partial u}{\partial t}+\left(u\frac{\partial u}{\partial x}+v\frac{\partial u}{\partial y}+w\frac{\partial u}{\partial z}\right)=\frac{\partial p'}{\partial x}+\frac{1}{Re_H}\left(\frac{\partial^2 u}{\partial x^2}+\frac{\partial^2 u}{\partial y^2}+\frac{\partial^2 u}{\partial z^2}\right)$ (3.8)

Component (Y):

$\frac{\partial v}{\partial t}+\left(u\frac{\partial v}{\partial x}+v\frac{\partial v}{\partial y}+w\frac{\partial v}{\partial z}\right)=\frac{\partial p'}{\partial y}+\frac{1}{Re_H}\left(\frac{\partial^2 v}{\partial x^2}+\frac{\partial^2 v}{\partial y^2}+\frac{\partial^2 v}{\partial z^2}\right)$ (3.9)

Component (Z):

$$\frac{\partial w}{\partial t}+\left(u\frac{\partial w}{\partial x}+v\frac{\partial w}{\partial y}+w\frac{\partial w}{\partial z}\right)=\frac{\partial p'}{\partial z}+\frac{1}{Re_H}\left(\frac{\partial^2 w}{\partial x^2}+\frac{\partial^2 w}{\partial y^2}+\frac{\partial^2 w}{\partial z^2}\right) \quad (3.10)$$

The modified pressure is $p'$, which is given by:

$$p'=p+\frac{2}{3}\rho.k \quad (3.11)$$

By using the eddy viscosity concept, the k-ε model is

$$\mu_{eff}=\mu+\mu_t \quad (3.12)$$

Where turbulence viscosity that denotes by $\mu_t$. The k-ε model posits a relationship between turbulence viscosity and turbulence kinetic energy and dissipation.

$$\mu_t=C_\mu.\rho.\frac{k^2}{\varepsilon} \quad (3.13)$$

Where the k-ε turbulent model constant is $C_\mu=0.09$.

The values of 'k' and 'ε' come straight from the turbulence kinetic energy, on the other hand, turbulence dissipation rate is from differential transmission equations.

$$\rho\left[\frac{\partial k}{\partial t}+\left(u\frac{\partial k}{\partial x}+v\frac{\partial k}{\partial y}+w\frac{\partial k}{\partial z}\right)\right]-\frac{\mu_{eff}}{\sigma_k}\left(\frac{\partial^2 k}{\partial x^2}+\frac{\partial^2 k}{\partial y^2}+\frac{\partial^2 k}{\partial z^2}\right)=P_k-\rho\varepsilon \quad (3.14)$$

$$\rho\left[\frac{\partial \varepsilon}{\partial t}+\left(u\frac{\partial \varepsilon}{\partial x}+v\frac{\partial \varepsilon}{\partial y}+w\frac{\partial \varepsilon}{\partial z}\right)\right]-\frac{\mu_{eff}}{\sigma_\varepsilon}\left(\frac{\partial^2 \varepsilon}{\partial x^2}+\frac{\partial^2 \varepsilon}{\partial y^2}+\frac{\partial^2 \varepsilon}{\partial z^2}\right)=\frac{\varepsilon}{k}(C_{\varepsilon 1}P_k-C_{\varepsilon 2}\rho\varepsilon) \quad (3.15)$$

Where the k-ε turbulent model constant is $C_{\varepsilon_1}=1.44$, $C_{\varepsilon_2}=1.92$, $\sigma_\varepsilon=1.3$

The following equation gives the shear productivity (Pk) due to disturbance for incompressible flow.

$$P_k=\mu_t\nabla\mathbf{U}\cdot(\nabla\mathbf{U}+\nabla\mathbf{U}^T)-\frac{2}{3}\nabla\cdot\mathbf{U}(3\mu_t\nabla\cdot\mathbf{U}+\rho k)+P_{k_b} \quad (3.16)$$

### 3.2. Conjugate heat transfer

A circular ground cooling pipe was modeled as a cross-flow heat exchanger with one fluid unmixed (i.e., air). An external thermal resistance was provided by a surrounding concentric

cylinder of the earth of arbitrary thickness, which was exposed to an undisturbed subsoil temperature as a boundary condition [53].

A steady-state analysis gives the thermal resistance ($R_s$) of the ‘‘soil annulus’’ as

$$R_s = \frac{\ln(r_1/r)}{2\pi Lk} \quad (3.17)$$

The thermal resistance ($R_c$) due to convection heat transfer between the air in the pipe and the pipe's inner surface may be expressed as

$$R_c = \frac{1}{2\pi rLh}, \quad (3.18)$$

where

$$h = \frac{N_u k_{air}}{d} \quad (3.19)$$

The convective heat transfer coefficient (h) in Eq. (3.18) above is a function of Reynolds number *Re*; and Nusselt number, $N_u$, where

$$Re = \frac{Vd}{v} \quad (3.20)$$

The total thermal resistance $R_{tot}$ between pipe air and surrounding soil of the EAHE system may then be determined from

$$R_{tot} = R_s + R_c \quad (3.21)$$

The overall coefficient of heat transfer is defined by

$$U = \frac{1}{R_{tot}}. \quad (3.22)$$

For a pipe of infinite length, the fluid (unmixed) through a constant temperature ($T_{\text{pipe surface}} = T_{(z,t)}$), the effectiveness of the EATHE can be defined as

$$\varepsilon = 1 - e^{-UA/\dot{m}C_p}, \quad (3.23)$$

where

$$\dot{m} = \rho\left(\frac{\pi d^2}{4}\right)V = q\rho.$$

The definition of temperature effectiveness ($\varepsilon$) is given by

$$\varepsilon = \frac{T_a - T_2}{T_a - T_{(z,t)}}. \quad (3.24)$$

Setting Eq. (3.23) equal to Eq. (3.24) and solving for ($T_2$); the exponential relation for an outlet air temperature of the earth–air heat exchanger as a function of the surrounding subsoil temperature ($T_{(z,t)}$) inlet air temperature ($T_a$) may be expressed as

$$T_2 = T_a - (T_a - T_{(z,t)})\varepsilon. \quad (3.25)$$

The total heat transferred to/from the air when flowing along the buried pipe may be expressed as

$$Q_1 = \dot{m}C_p(T_a - T_2). \quad (3.26)$$

# 4. Chapter: Numerical Method

## 4.1. System description and simulation setup

Thermal analysis has been utilized to assess an EATHE system's thermal performance (under transient conditions). Numerical simulations are determined using a CFD model. It may predict fluid flow that is turbulent, laminar, compressible, or incompressible, as well as fluidity and compressibility events. FLUENT models may capture turbulence behavior close to walls by using enlarged wall functions. [39].

### 4.1.1. Physical model

**Figure 8** shows the geometrical model of EATHE systems, the PVC pipe, surrounding soil, and other materials used for modeling. The input parameters are: pipe diameter is 0.1m, pipe length 60m, soil thermal conductivity of 1.25$Wm^{-1}K^{-1}$, and air velocity 3$ms^{-1}$. Observations were made of the physical model of the EATHE system in summer weather conditions as shown in June 2011 in Ajmer (Western India)

**Figure 8**: Experimental setup of EATHE system[42].

### 4.1.2. Simulation model

All the geometric parameters are the same as in the existing experimental setup in **Table 1**. The simulation model of the straight EATHE system is meshed using 3D hybrid (hexahedral and tetrahedral) mesh networks (**Figure 9**), consisting of a total of 2,326,116 cells (elements). The governing equations are converted numerically, and the solution procedure of algebraic equations is used in this work. The finite volume approach is used in this work. The numerical answers are based on the assumptions listed below:

i. Soil thermal conductivity, PVC pipe, and air velocity (v) remain constant during the operation.

ii. Because of the fluctuation in soil temperature surrounding them, the vertical pipes are properly insulated and do not affect the air temperature.

iii. No effect of moisture.

iv. Within each section close to the tube of an EATHE, the air mixes uniformly without strata.

v. The initial assumptions make the soil and PVC pipe temperatures uniform and undisturbed.

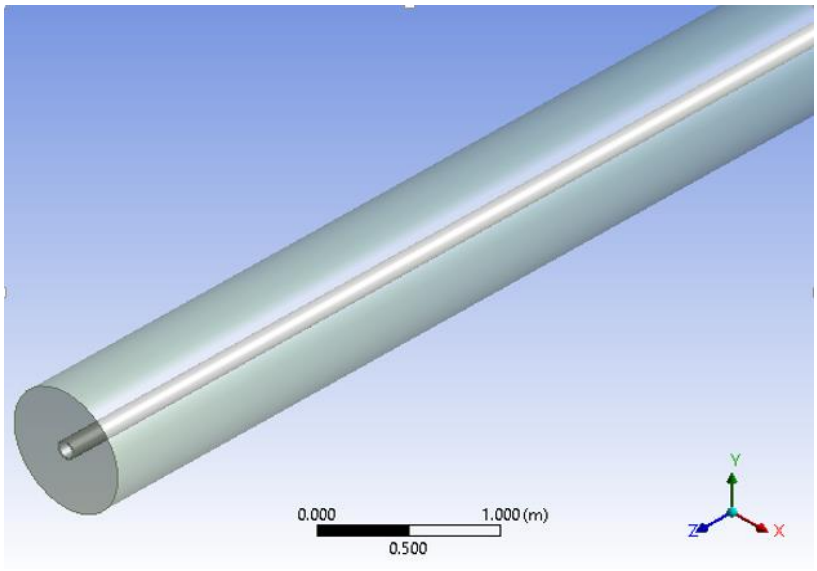


**Figure 9**: Modeling of EATHE

### 4.2. Boundary conditions

The boundary conditions that are applied for the analysis -

i. Inlet conditions: At the EATHE inlet, a uniform velocity is utilized, and the direction is normal to the opening. The velocity (v) along the x-axis is set at 3 m/s, and the temperature is 319K. 5 percent turbulence intensity and a 0.1 m inlet characteristic length (hydraulic diameter) is calculated as Turbulence parameters.

ii. Soil far boundary: The outside surface of the soil around the EATHE pipe (10 times the pipe diameter) assumed a constant temperature of 300.2 K.

iii. Inlet & exit face: A zero-heat flux condition is assumed at both the input and outflow faces of the EATHE pipe.

iv. Outlet condition: Outlet condition is typical for pressure outlet, and backflow direction is normal to the boundary. Radial equilibrium pressure distribution is off.

v. Interface condition: As previously stated, coupled heat transport is expected at the soil-pipe contact. Constant temperatures and no-slip criteria for velocity are used at the duct surfaces. All flow variables have a zero-diffusion flux in the outlet direction.

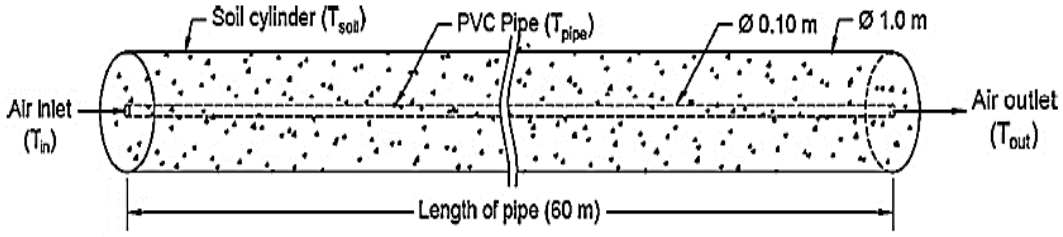


**Figure 10**: Computational domain for 60m long pipe.

The soil environment in the far-field was handled as fixed temperature zones. Moreover, the soil conditions are treated as constant. In the worst case, it had been performed by different simulations, and the ground temperature does not fluctuate considerably over a certain distance. Once it reaches 10 times the pipe diameter, the distance may be disregarded. [47].

**Table 1**: Geometric parameters of the EATHE system

| SL | Input parameters | Values |
|---|---|---|
| 1 | Pipe Diameter (m) | 0.1 |
| 2 | Pipe length (m) | 60 |
| 3 | Air velocity ($ms^{-1}$) | 5 |
| 4 | Surrounding temperature of soil (K) | 300.2 |
| 5 | Thermal conductivity of soil ($W\ m^{-1}\ K^{-1}$) | 1.25 |
| 6 | Soil thermal diffusivity ($m^2s^{-1}$) | 0.00232 |

In this study, a PVC pipe with an inlet diameter of 0.1m, a thickness of 0.005m, and an outer diameter with soil is 1.1 m is considered a total control volume. Modeling was done for this control volume for the analysis. The pipe's outer surface and surrounding soil layer were "Coupled" so that they could initiate heat transfer, and initial conditions are set as shown in **Table 1.**

**Table 2**: The physical and thermal characteristics of the various simulated materials

| SL | Material | Density ($kg\ m^{-3}$) | Specific heat capacity ($J\ kg^{-1}\ K^{-1}$) | Thermal conductivity ($W\ m^{-1}\ K^{-1}$) |
|---|---|---|---|---|
| 1 | Air | 1.225 | 1.006 | .024 |
| 2 | PVC | 1380 | 900 | 1.16 |
| 3 | Soil-1 | 2050 | 1840 | .65 |
| 4 | Soil-2 | 2050 | 1840 | 1.25 |
| 5 | Soil-3 | 2050 | 1840 | 3.5 |

This research looked into the impact of soil thermal conductivity and other geometric parameters like pipe length, pipe thickness, the thermal performance of EATHEs, and so on. An approved three-dimensional transient numerical model was used to conduct the inquiry. ANSYS FLUENT

was used to do the transient analysis. There have some constant on physical materials that showed in **Table 2**. The output air temperature is used to evaluate the performance. The findings have been validated against experimental data and can be used in any study involving EATHE.

### 4.3. Numerical procedure

Discretization of the governing equations is the initial step of the numerical simulation. Discretization aims to reduce the governing partial differential equations to a set of algebraic equations. The Finite Volume Method (FVM) is used in this Computational Fluid Dynamics (CFD) code. This method discretizes the spatial domain into finite control volumes using the mesh. The governing equations are integrated across each control volume, resulting in discrete conservation of significant quantities (mass, momentum, and energy) for each control volume. The solver quickly corrects local faults in the solution. An algebraic multi-grid technique is employed to speed up solver convergence by computing corrections on coarse grid levels. The momentum and energy equations are discretized using the second order upwind approach in all simulations.

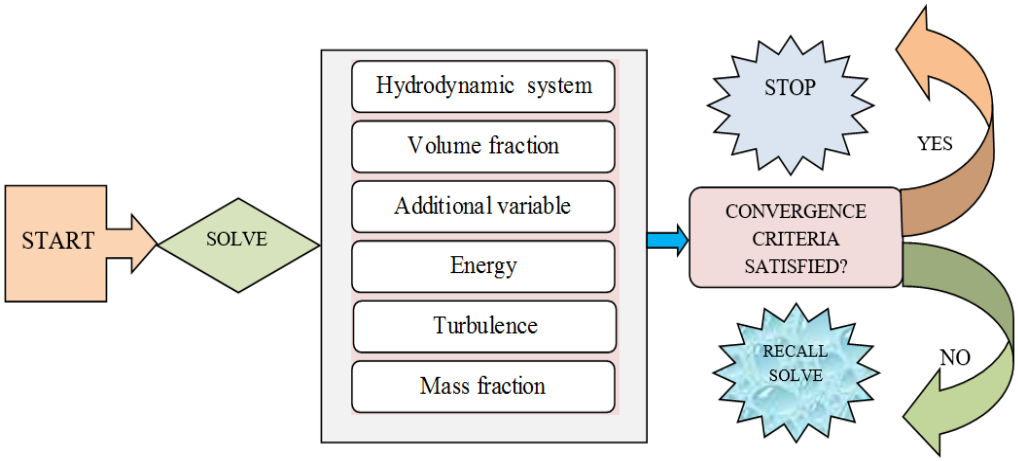


**Figure 11**: Numerical procedure

The hydrodynamic equations (for u, v, w, and p) are solved as a single system using this algorithm, which employs a coupled solver. The number of repetitions necessary to reach a

steady state is reduced. The solution technique is depicted in the flow chart below. Each set of equations is solved using two numerically expensive processes.

i. The non-linear equations are linearized (coefficient iteration) and combined into the solution matrix for each time step.

ii. An algebraic multi-grid approach is used to solve the linear equations (equation solution iteration).

The physical time step or local time step factor option controls the time step iteration to progress the solution in time for a steady state simulation. There is only one linearization iteration per time step in this situation.

### 4.4. Convergence

It is advised that a target variable of monitoring the numerical inaccuracy to achieve the necessary precision. The numerical scheme's convergence may be tested quickly and without the need for interpolation between grids. There are several viewpoints on how to assess convergence. The residual measures each of the conservative control volume equation. It is the most crucial criterion for convergence since it directly relates to whether or not the equations have been solved. The CFD algorithm shows the normalized residuals to evaluate convergence. Convergence is measured consistently by normalizing the residuals, and an average normalized residual of $1e^{-6}$ to $1e^{-7}$ is always very close to the precision of the machine's rounding off. When a preset level is reached, the normalized residual is utilized to end the solver automatically. Only the spatial flux terms are used to construct this residual. The decrease in residuals is the first indicator of the solution's convergence to a steady state. Various types of flows need varying degrees of residue reduction. Plotting the residuals for each equation after each time step can be used to determine how well the solution has converged.

### 4.5. Grid sensitivity study

A grid sensitivity test is necessary to get the appropriate degree of accuracy with the minimal possibility of computing time. The amount of time required for computing increases with the number of elements. Therefore, a more refined grid may not always be the best option. On the other side, a coarser grid may cause inaccurate results. Three alternative grid sizes were used in grid sensitivity testing to see whether the computation was acceptable. **Table 3** shows the nodes and elements that take the condition curvature.

In this study, it was assumed that air is incompressible, that the soil is homogenous, and has constant physical qualities. It was also assumed that the pipes and ground materials properties do not vary with temperature and that the CFD model's engineering materials are isotropic and homogenous. The study applied the standard fluid dynamics and heat transport formulas. The geometry was modeled and meshed in ANSYS 19.0. In this work, an unstructured grid was used for the CFD simulations shown in **Figure 12**.

**Table 3**: Different grid resolutions for 60 m long pipe

| 60 m long pipe configuration | No of nodes | No of elements |
|---|---|---|
| Test 1(coarse mesh) | 1461467 | 1432382 |
| **Test 2 (medium mesh)** | **1816920** | **1785240** |
| Test 3(fine mesh) | 2263318 | 1993342 |

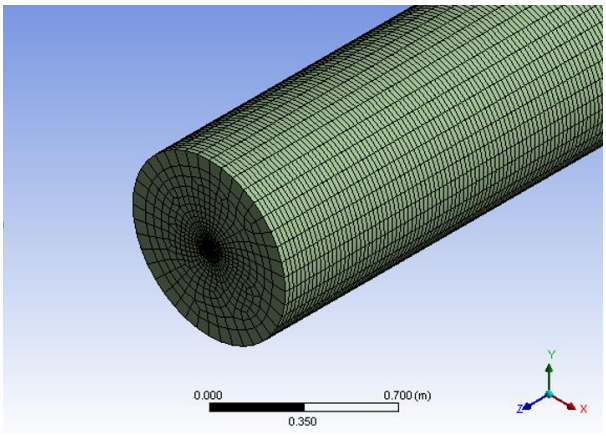


(a)

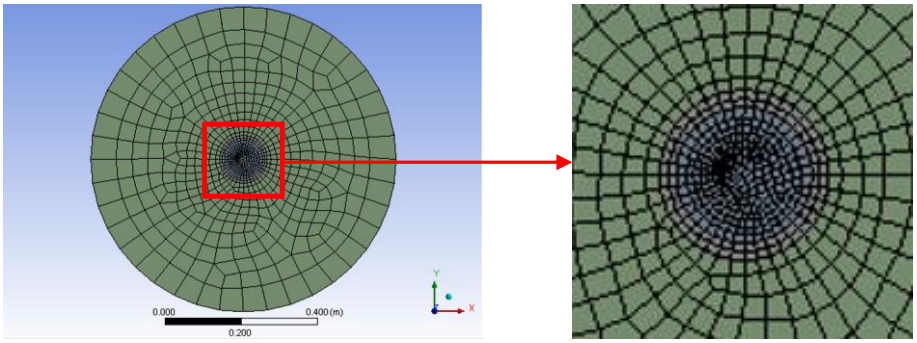

(b)

**Figure 12**: Schematic diagram of meshing body (a) Meshing (side view) (b) Meshing (front face).

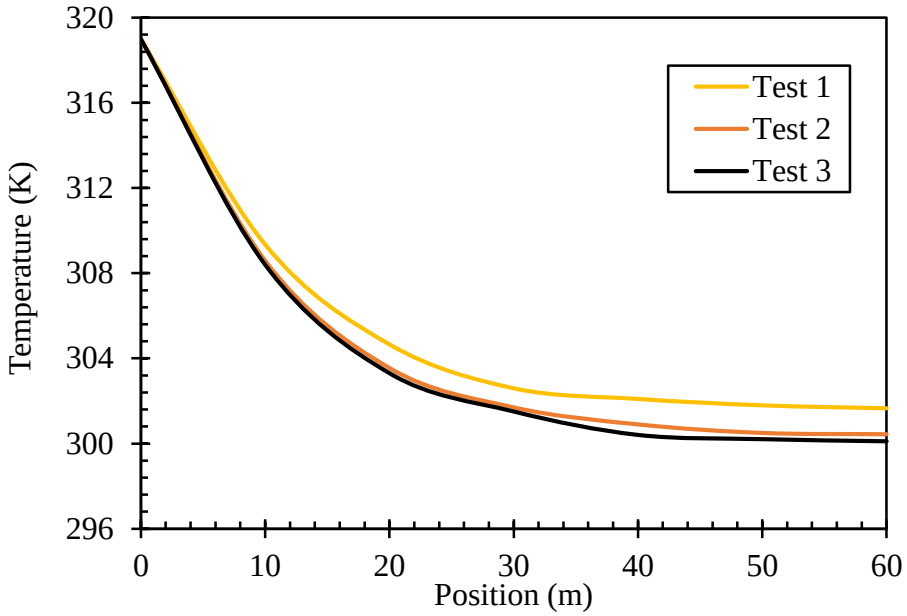


**Figure 13**: Grid Independence Test: Simulated air temperature along pipe length for fine, medium, and coarse mesh.

A grid-independent test, **Figure 13** and **Table 3,** was carried out to confirm the impact of mesh size on the solution's accuracy. Mesh sizes between the pipe surface and the outer soil layer range from 0.015 to 0.075 meters. Following improvements, the independent grid size was determined, increasing the number of elements from 14, 32,382 (coarse mesh) to 19, 93,342 (fine mesh). The outer diameter of the soil cylinder that surrounds the EATHE pipe has been calculated to be ten times that of the pipe. To test this theory, a CFD simulation is examined to develop an EATHE model with a 60 m pipe length and 0.1 m pipe diameter. The radius of the earth around the pipe was calculated to be 10 times the pipe radius, Test 1(coarse mesh), Test 2 (medium mesh) and

Test 3(fine mesh) is the basic comparison of the different grids and their trends were presented in **Figure 13**. The trend line for Test 2 is 8.58% more effective by Test 1, it also show that Test 3 give 1.44% significant result from Test 2.

### 4.6. Model validation

The performance of the EATHE system was evaluated by running it continuously throughout the year in the selected experimental setup. The thermal performance of the EATHE system under steady-state conditions has been considered to validate the CFD simulation model and findings. The CFD model for EATHE system steady analysis was verified for summer weather conditions by obtaining observations on a full-scale experimental set-up as depicted in **Figure 14** for June 2011 in Ajmer (Western India). The input parameters for experimental and theoretical research in depth are shown in **Table 4.** The air inlet condition in the CFD simulation was kept the same as measured in the experimental set-up for this validation exercise. A pipe with a diameter of 0.3 m and a length of 24.7 m was created to validate the EATHE model.

**Table 4**: Input parameters for comparative validation

| SL | Parameters | Unit |
|---|---|---|
| 1 | Pipe diameter | 30 cm |
| 2 | Pipe length | 24.7m |
| 3 | Air velocity | 1.5 $ms^{-1}$ |
| 4 | Soil temperature | 291.8K |
| 5 | Pipe depth | 2.13m |
| 6 | Soil thermal conductivity | 1.16$Wm^{-1}K^{-1}$ |
| 7 | Soil thermal diffusivity | 0.00232 $m^2s^{-1}$ |

**Table 5:** Simulation model validation (ambient air temperature: 25.56 $^{0}$C).

| Axial distance from the EATHE pipe inlet (m) | Experimental data (K) [54] | Theoretical data (K) [53] | simulation model (K) |
|---|---|---|---|
| 3.35 | 298 | 297.94 | 298.01 |
| 6.4 | 297 | 297.43 | 297.7 |
| 9.45 | 298 | 296.97 | 297.52 |
| 12.5 | 297 | 296.54 | 296.9 |
| 15.55 | 296.8 | 296.15 | 296.56 |
| 24.7 | 296.8 | 295.16 | 295.65 |

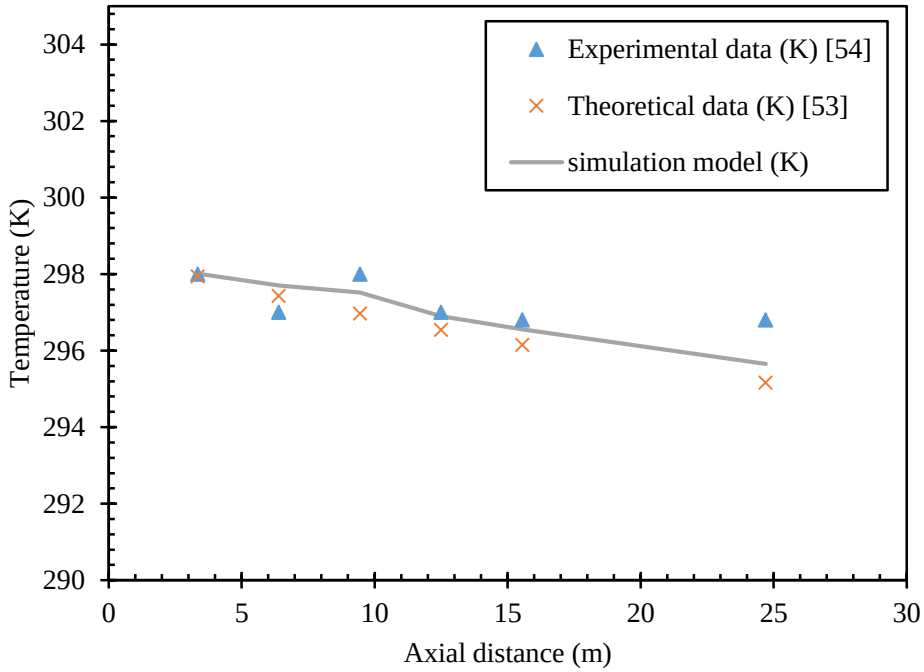


**Figure 14**: Experimental [54], theoretical [53], and simulated data for model validation.

The figure illustrates that the difference between the experimental value and the simulated value for the dry bulb temperature of the air in the middle of the pipe is 3.4% to 8.0%. Thus, the model was considered to carry out our detailed analysis. The previous section's model was tested against theoretical models and experimental data from other researchers, in addition to comparisons to self-experimental results. Al-Ajmi et al. [53] established the theoretical model for the

comparison, which was tested against relevant experimental and theoretical investigations. Mathur [54] conducted an empirical study in North Carolina using a pipe diameter of 30 cm, a pipe length of 24.7 meters, and a pipe depth of 1.7 meters.

**Table 5** and **Figure 14** show the practical and theoretical research outcomes. The values from both studies are considered, and it is clear that the results are consistent with one another. However, there are only minor discrepancies between the simulation model and the Al-Ajmi model, suggesting the model is reliable for predicting an EATHE system's behavior.

# 5. Chapter: Results and Discussion

The current investigation is performed to study the effect of the thermal conductivity of soil, the velocity of air entering the EATHE (inlet air velocity), thickness, and length of the PVC pipe on the thermal performance of the EATHEs. The performance of EATHEs was tested in terms of the temperature drop detected at the outlet portion of the EATHE using 3-D simulations and the k-epsilon model. As the temperature decreases, EATHE functions more effectively. Initially, the current study analyzes the thermal performance based on three different soil samples with different thermal conductivity values. Samples 1, 2, and 3 have a thermal conductivity of 0.65 $Wm^{-1}K^{-1}$, 1.25 $Wm^{-1}K^{-1,}$ and 3.5 $Wm^{-1}K^{-1,}$ respectively. The soil temperature at a depth of 3.7m was found to be 300.24K, and it was assumed to be a constant [38] during the whole operation of the EATHE. It is known as the undistributed soil temperature, as it remains unaffected by the environmental temperature above the soil surface. Although there is heat generation for soils with low thermal conductivity, and the temperature does not remain constant anymore, we assumed it to stay consistent. This heat generation in the case of soil with low thermal conductivity will result in a deteriorated thermal performance.

Since the thickness of the PVC pipe affects the thermal performance, it is a crucial parameter for financial consideration, and this impact is studied over a range of air velocities entering the EATHE, from 3 $ms^{-1}$ to 6 $ms^{-1}$. Another parameter related to economic operation is the length of the PVC pipe. Bansal et al. [38] reported on comparative research into the application's appropriateness of the turbulence model. However, his investigation was limited to the horizontal plane PVC pipe. The present study investigates the effect of different geometric parameters, pipe cross-section, the inclusion of fins on the pipe, and the pitch of multiple pipe arrangements on the thermal performance of EATHEs under steady and transient conditions. All simulations are

performed with a 60 m pipe length to determine how much shorter the pipe may be without negatively impacting its thermal performance.

### 5.1. Soil layer variations in different configurations

The current investigations and works have been conducted considering the air duct length of 60 m PVC material. The exact output temperature is achieved for varying soil thicknesses around the PVC pipe when air is forced into the duct at 3m/s to transfer heat from 319K ambient temperature. Investigation takes different types of soil layers like eight times, ten times, and 15 times for a constant thermal conductivity of 3.5 $Wm^{-1}K^{-1}$ with a constant air velocity of 3.5m/s. Fluent analysis of turbulent airflow 3m/s passing through a 60m long PVC pipe at different soil layers was conducted to determine the air outlet temperature. The results are tabulated in **Table 6** for the temperature at different lengths. **Figure 15** shows the outlet Temperatures profile cross-section for soil conductivity of 3.5 W/mK and inlet air velocity of 3m/s with varying soil thickness (a). Soil 8 times, (b). Soil 10 times, and (c). Soil 15 times.

**Table 6:** Thermal effect of air for different soil layers with 3.5 $Wm^{-1}K^{-1}$ thermal conductivity and 3$ms^{-1}$ air velocity.

| **SL** | Soil layers | **Position(m)** | | | | | | |
|---|---|---|---|---|---|---|---|---|
| | | 0 | 10 | 20 | 30 | 40 | 50 | 60 |
| | | Temperature (K) | | | | | | |
| **1** | 8 times | 319 | 308.4 | 303.3 | 301.5 | 300.4 | 300.2 | 300.1 |
| **2** | 10 times | 319 | 308.3 | 303.2 | 301.4 | 300.4 | 300.2 | 300.1 |
| **3** | 15 times | 319 | 308.2 | 303.1 | 301.3 | 300.4 | 300.2 | 300.1 |

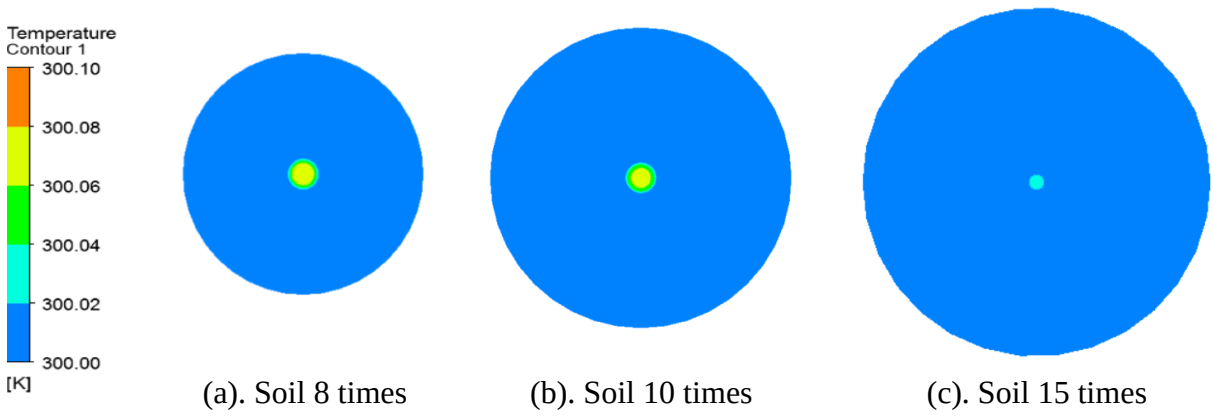


(a). Soil 8 times (b). Soil 10 times (c). Soil 15 times

**Figure 15:** Outlet Temperatures of the cross-section for soil conductivity 3.5 $Wm^{-1}K^{-1}$ and inlet air velocity 3m/s with varying soil thickness (a). Soil 8 times, (b). Soil 10 times and (c). Soil 15 times.

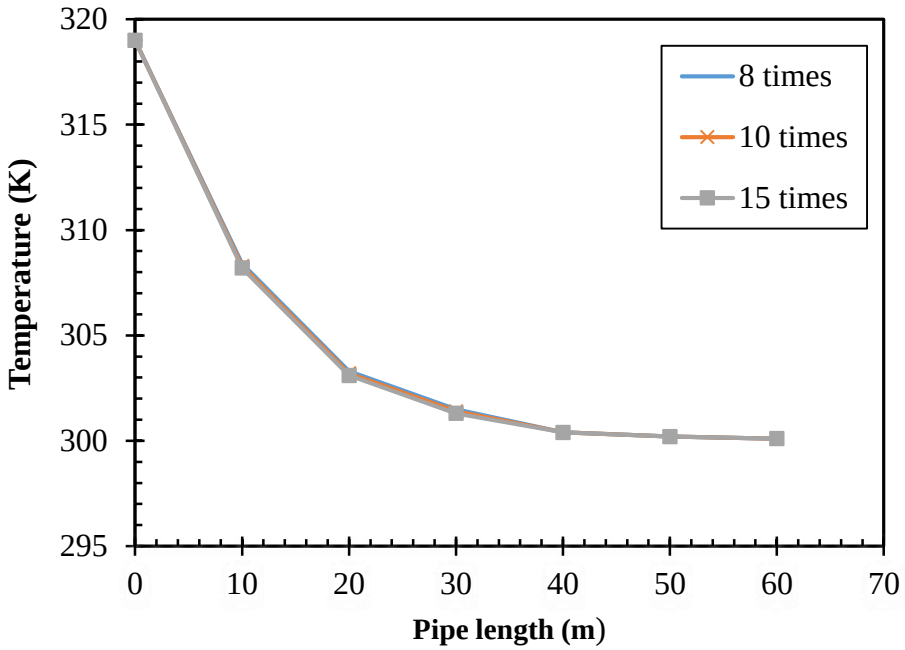


**Figure 16:** Thermal effect of air soil thickness for soil conductivity 3.5 $Wm^{-1}K^{-1}$ and inlet air velocity 3m/s

The air domain remains at higher temperature when the pipe is in its initial position. The temperature contour cross-section of the PVC in **Figure 16** shows a relative temperature drop from the center of the duct to the soil domain where soil temperature remains constant.

### 5.2. Effect of thermal conductivity in a different setup

The current study analyzes the thermal performance based on three different soil samples, each having a different thermal conductivity value. Sample 1, 2 and 3 has, thermal conductivity, 0.65 $Wm^{-1}K^{-1}$, 1.25 $Wm^{-1}K^{-1}$ and 3.5 $Wm^{-1}K^{-1}$. In this investigation, CFD analysis takes homogeneous inlet air velocities $3ms^{-1}$, $4ms^{-1,}$ and $5ms^{-1}$; EATHE has been conducted to visualize the temperature drop trends in lesser pipe lengths. In the course of EATHE's research, several experiments with PVC pipes of varying lengths have been conducted, and it has been determined that the initial 40 meters of a 100-meter pipe account for about 83.5 percent of the total temperature drop of the working fluid, while the value changes to 90 percent at the 50-meter mark. This conclusion indicates a significant portion of the heat transfer occurs in the first half of the pipe. A similar CFD analysis in this investigation taking homogeneous soil of thermal conductivity 3.5, 1.25, and 0.65 $Wm^{-1}K^{-1}$ around the buried EATHE has been conducted to visualize the temperature drop trends in lesser lengths of the pipe.

#### 5.2.1. For 60 meter long pipe soil ten times 0.65 $Wm^{-1}K^{-1}$

In this research, the air outlet temperature was calculated using a computational fluid dynamics (CFD) simulation of a turbulent airflow at varying velocities traveling through a 60-meter-long pipe with a uniform soil layer, assuming that it is ten times the hydraulic diameter. The results are tabulated in **Table 7** of temperature at different lengths. **Figure 17** shows the temperature trend line along the length for other flows at soil thermal conductivity of 0.65 $Wm^{-1}K^{-1}$.

**Table 7:** Thermal effect of air for 60m long pipe with thermal conductivity 0.65 $Wm^{-1}K^{-1}$.

| SL | Velocity | Position (m) | | | | | | |
|---|---|---|---|---|---|---|---|---|
| | | 0 | 10 | 20 | 30 | 40 | 50 | 60 |
| | | Temperature (K) | | | | | | |
| **1** | 5m/s | 319 | 314.35 | 310.77 | 307.93 | 305.87 | 304.21 | 303.18 |
| **2** | 4m/s | 319 | 313.61 | 309.53 | 306.73 | 304.77 | 303.34 | 302.23 |
| **3** | 3m/s | 319 | 312.65 | 308.18 | 305.17 | 303.33 | 302.13 | 301.29 |

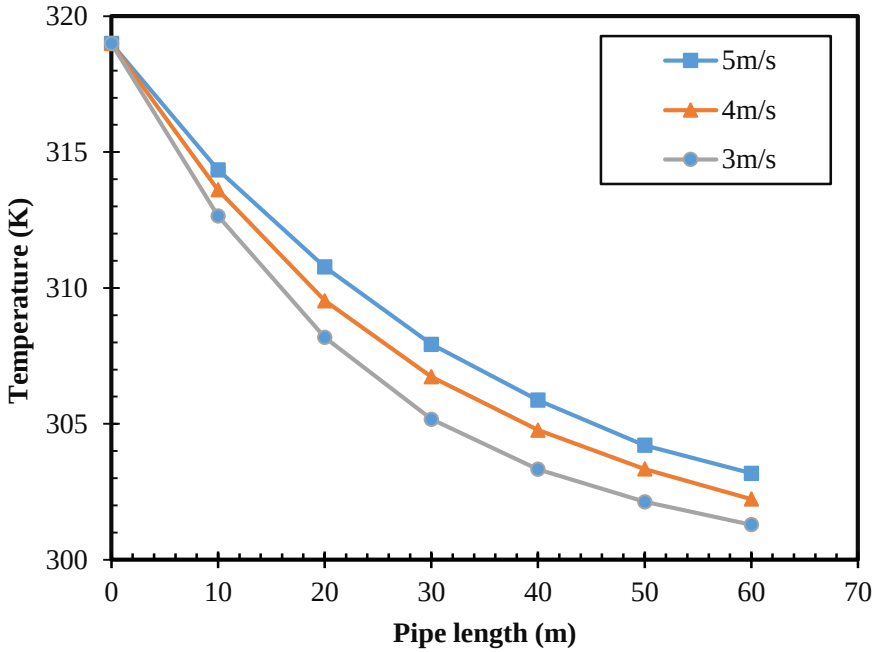


**Figure 17:** Temperature trend line along the length for different flows at soil thermal conductivity of 0.65 $Wm^{-1}K^{-1}$.

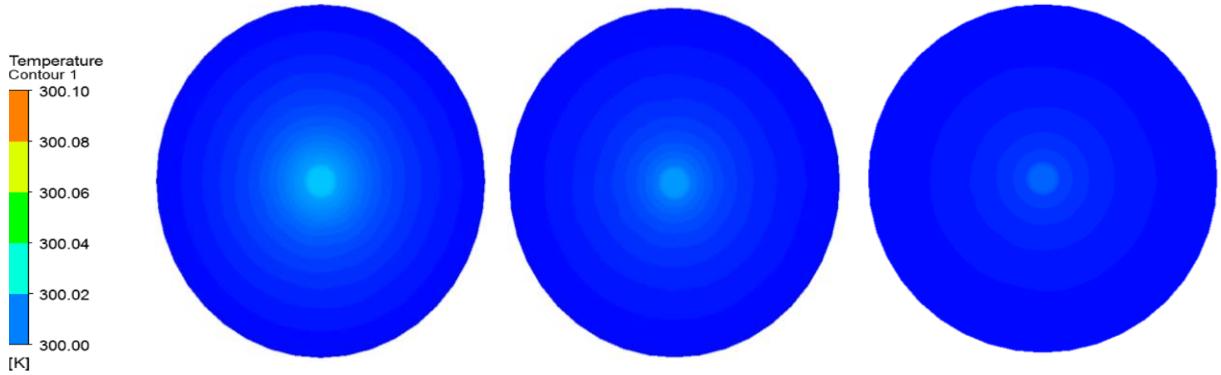


(a). 5m/s (b). 4m/s (c). 3m/s

**Figure 18:** Outlet Temperatures profile for different flow (a). 5 m/s, (b). 4 m/s, and (c). 3 m/s for soil conductivity 0.65 $Wm^{-1}K^{-1}$.

Also, the temperature contour cross section in **Figure 18** of the PVC shows a relative temperature drop from the center of the duct to the soil domain, where soil temperature remains constant. Air domain remains at a higher temperature when the velocity is higher as the working fluid gets less time to dissipate energy to the soil with a lower temperature. The outlet temperature is 303.18K for velocity $5ms^{-1}$ and 301.29K for $3ms^{-1}$. A vital indication from the figure shows the outlet temperature, which is the lowest for the slowest air velocity. The thermal

conductivity of soil plays the most significant role in heat transfer from the air as it determines how fast soil can absorb thermal energy from air passing through the pipe.

### 5.2.2. For 60 meter long pipe soil ten times 1.25 $Wm^{-1}K^{-1}$

CFD analysis of turbulent airflow at various speeds the temperature of the air exiting a 60-meter-long pipe was calculated using a uniform soil layer that is 10 times the hydraulic diameter and thermal conductivity of 1.25 Wm-1K-1. The thermal effect of air for 60 m long pipe with thermal conductivity 1.25 $Wm^{-1}K^{-1}$ is tabulated in **Table 8** of temperature at different lengths.

**Table 8:** Thermal effect of air for 60m long pipe with thermal conductivity 1.25 $Wm^{-1}K^{-1}$.

| SL | Velocity | Position(m) | | | | | | |
|---|---|---|---|---|---|---|---|---|
| | | 0 | 10 | 20 | 30 | 40 | 50 | 60 |
| | | Temperature (K) | | | | | | |
| **1** | 5m/s | 319 | 312.62 | 308.05 | 305.07 | 303.22 | 302.04 | 301.229 |
| **2** | 4m/s | 319 | 311.72 | 306.94 | 304.06 | 302.41 | 301.44 | 300.76 |
| **3** | 3m/s | 319 | 310.65 | 305.55 | 302.94 | 301.58 | 300.88 | 300.37 |

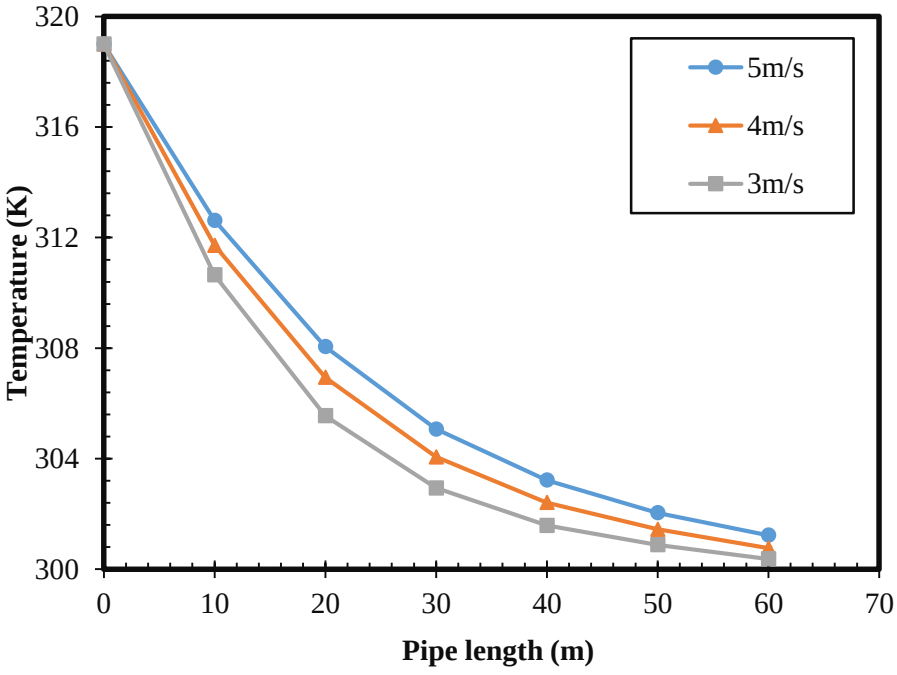


**Figure 19:** Temperature trend line along the length for different flows at soil thermal conductivity of 1.25 $Wm^{-1}K^{-1}$

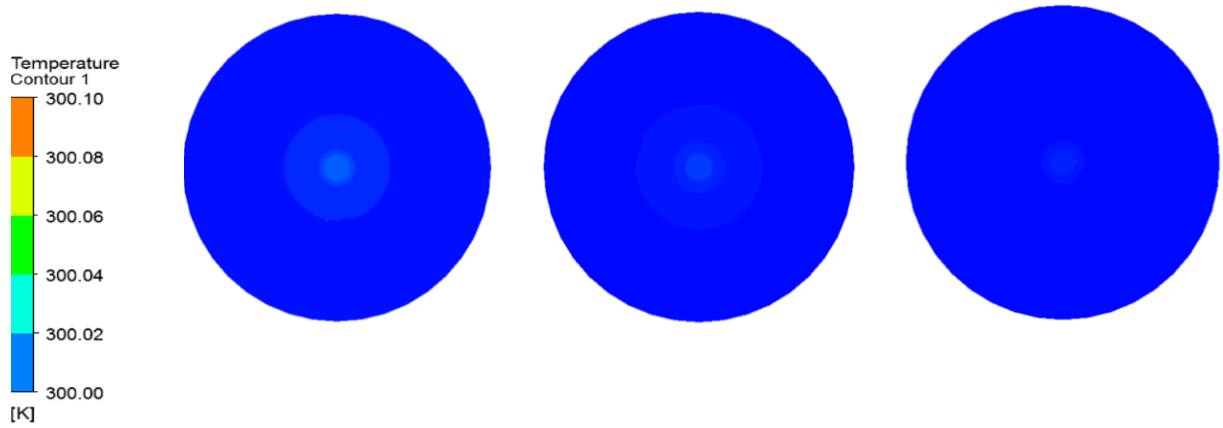


(a). 5m/s (b). 4m/s (c). 3m/s

**Figure 20:** Outlet Temperatures profile for different flow (a). 5 m/s, (b). 4 m/s, and (c). 3 m/s for soil conductivity 1.25 $Wm^{-1}K^{-1}$

A similar trend is observed in a better heat transfer medium. At soil conductivity of 1.25 $Wm^{-1}K^{-1}$ the outlet temperature drops lower relative to the drop in soil with conductivity 0.65 $Wm^{-1}K^{-1}$. This is evidence of the effect of thermal conductivity on the cooling room air by absorbing the heat at a proportional rate. The Air domain remains at a higher temperature when the velocity is higher as the working fluid gets less time to dissipate energy to the soil at a lower temperature. The outlet temperature is 301.229K for velocity $5ms^{-1}$ and 300.37K for $3ms^{-1}$. An important indication noticed from the **Figure 19** is that the outlet temperature is the lowest for the slowest air velocity. Also, the temperature contour cross section given in **Figure 20** of the PVC shows a relative temperature drop from the center of the duct to the soil domain where soil temperature remains constant. The thermal conductivity of soil plays the most significant role in heat transfer from the air as it determines how fast soil can absorb thermal energy from air passing through the pipe.

### 5.2.3. For 60 meter long pipe soil ten times 3.5 $Wm^{-1}K^{-1}$

**Table 9** displays the temperature at different lengths of the PVC when the EATHE is placed in soil of thermal conductivity of 3.5 $Wm^{-1}K^{-1}$. The expected result is obtained in the initial measurements, but the degradation slope deteriorates in the second half of the EATHE. The drop in temperature in the exit portion is negligible and doesn't vary to a noticeable extent when conductivity increases or pipe length increases.

**Table 9:** Thermal effect of air for 60m long pipe with thermal conductivity 3.5 $Wm^{-1}K^{-1}$.

| SL | Velocity | Position(m) | | | | | | |
|---|---|---|---|---|---|---|---|---|
| | | 0 | 10 | 20 | 30 | 40 | 50 | 60 |
| | | Temperature(K) | | | | | | |
| **1** | 5m/s | 319 | 310.08 | 304.97 | 302.45 | 301.16 | 300.5 | 300.23 |
| **2** | 4m/s | 319 | 309.2 | 304.1 | 301.8 | 300.8 | 300.3 | 300.1 |
| **3** | 3m/s | 319 | 308.2 | 303.1 | 301.2 | 300.4 | 300.2 | 300.1 |

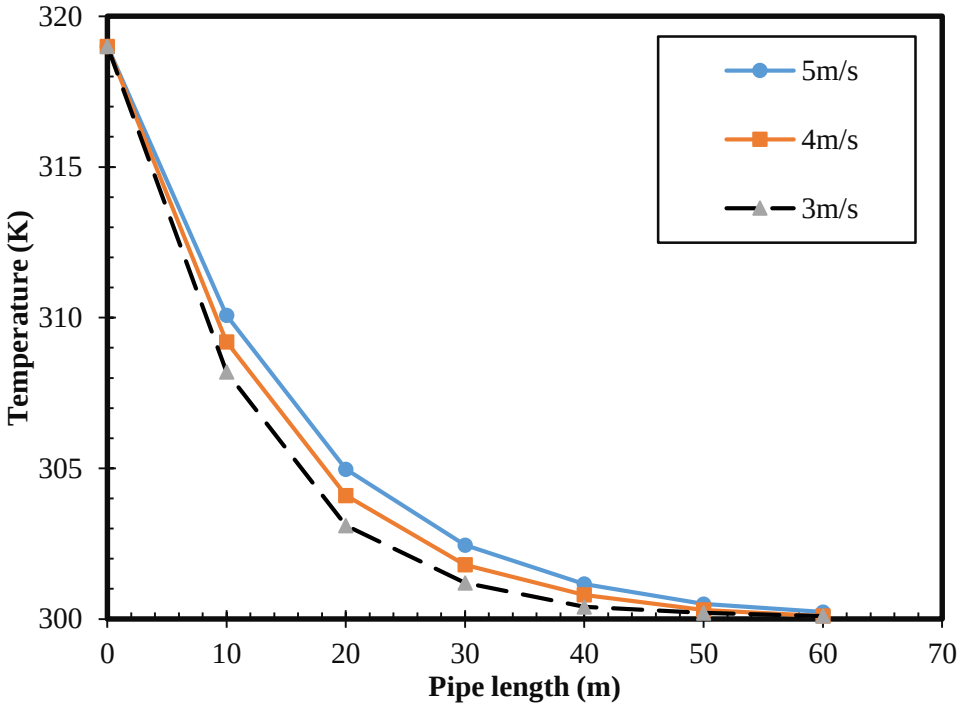


**Figure 21:** Temperature trend line along the length for different flows at soil thermal conductivity of 3.5 $Wm^{-1}K^{-1}$

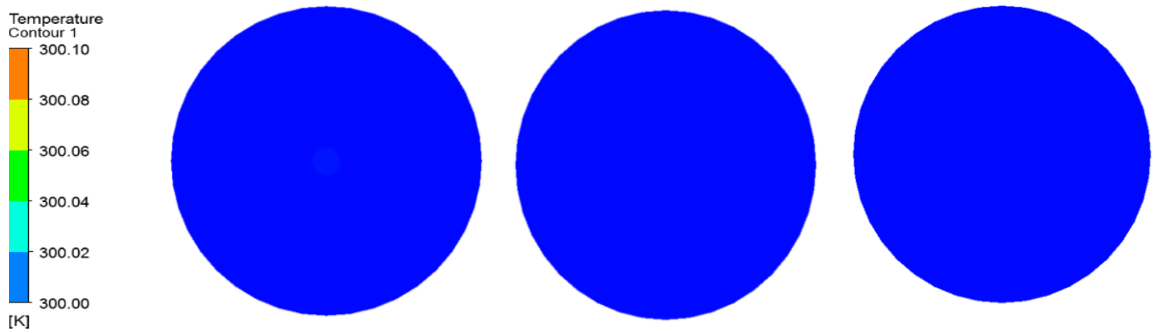


(a). 5m/s (b). 4m/s (c). 3m/s

**Figure 22:** Outlet Temperatures profile for different flow (a). 5 m/s, (b). 4 m/s, and (c). 3 m/s for soil conductivity 3.5 $Wm^{-1}K^{-1}$

An important indication noticed from the **Figure 21** shows that the outlet temperature is the lowest for the slowest air velocity. The temperature contour cross section given in **Figure 22** of the PVC shows a relative temperature drop from the center of the duct to the soil domain where soil temperature remains constant. Investigation of the critical factors impacting an EATHE's thermal performance resulted in developing techniques that increase effectiveness and achieve lower air temperatures. By adding an external heat transfer region, the EATHE may be improved with the optimal settings established. The Air domain remains at a higher temperature when the velocity is higher as the working fluid gets less time to dissipate energy to the soil at a lower temperature. The outlet temperature is 300.23K for velocity $5ms^{-1}$ and 300.1K for $3ms^{-1}$. The best result is obtained with the highest thermal conductivity and lowest inlet air velocity because of the proportional relation of air particle to pipe wall interaction time and heat transfer rate.

### 5.3. Effect of fin distance on the heat transfer performance

Numerous configurations of the EATHE were numerically simulated to examine the impacts of fins and other materials, and the performance was assessed using the outlet temperature. EATHE uses the pipe boundary wall to restrict the airflow carrying heat from the room to dissipate to the soil, thus recirculating cooler air to the intended area. So, the general understanding is that the increment of constrictions will result in lower outlet temperature. Fins of 10 mm thickness have been added to the inner wall of the intake side at various numbers and spacings to fit this restriction. The impact of fins was investigated initially by installing a single 10 mm fin at 0.5 m, which caused the output temperature to be 306.7 K, albeit this figure was reduced to 306.5 K with the addition of a second fin at 1 m. Four fins, measured from the entrance at 0.5, 1 m, 1.5 m, and 2 m, respectively, help the temperature decline with time. With this new feature, the outlet temperature is 306.1K, which is 19.4% higher than the straight EATHE without fins.

#### 5.3.1. 10 meters extended pipe fin use after 0.5 m distance

CFD analysis of turbulent airflow of 3m/s velocities of a ten meter extended pipe, a uniform soil layer is considered ten times from hydraulic diameter, and thermal conductivity of 3.5 $Wm^{-1}k^{-1}$ was conducted to determine the outlet temperature of the air. The Thermal effect of air temperature in length with fins every 0.5 m is shown in Table **10.**

**Table 10:** Thermal effect of air temperature in length with fins every 0.5m

| SL | No of fin | Position (m) | | | | | | | | | | |
|---|---|---|---|---|---|---|---|---|---|---|---|---|
| | | 0 | 1 | 2 | 3 | 4 | 5 | 6 | 7 | 8 | 9 | 10 |
| | | Temperature(K) | | | | | | | | | | |
| **1** | 1fin | 319 | 316.5 | 315.3 | 314.5 | 312.6 | 311.3 | 310.2 | 309.1 | 308.2 | 307.4 | 306.7 |
| **2** | 2fins | 319 | 316.3 | 315.1 | 314.3 | 312.4 | 311.1 | 310 | 308.9 | 308 | 307.2 | 306.5 |
| **3** | 3fins | 319 | 316.1 | 314.9 | 314.1 | 312.2 | 310.9 | 309.8 | 308.7 | 307.8 | 307 | 306.3 |
| **4** | 4fins | 319 | 315.9 | 314.7 | 313.9 | 312 | 310.7 | 309.6 | 308.5 | 307.6 | 306.8 | 306.1 |

An important indication noticed from the **Figure 23** shows that the outlet temperature is the lowest for increasing the number of the fin. When the number of fin increases, the surface area increases and obstructs airflow. As a result, inlet air takes time to drop the temperature.

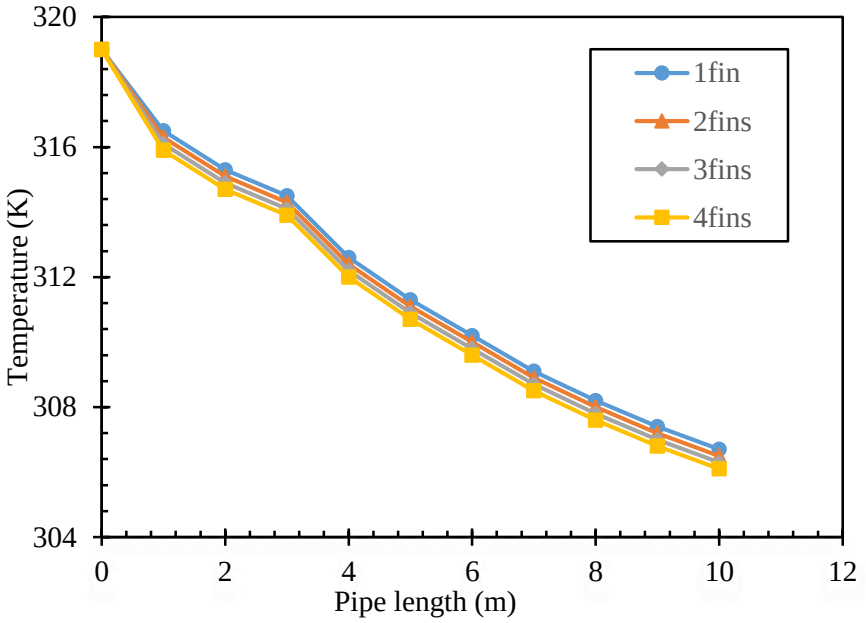


**Figure 23:** Temperature trend line length for different fins every 0.5 m.

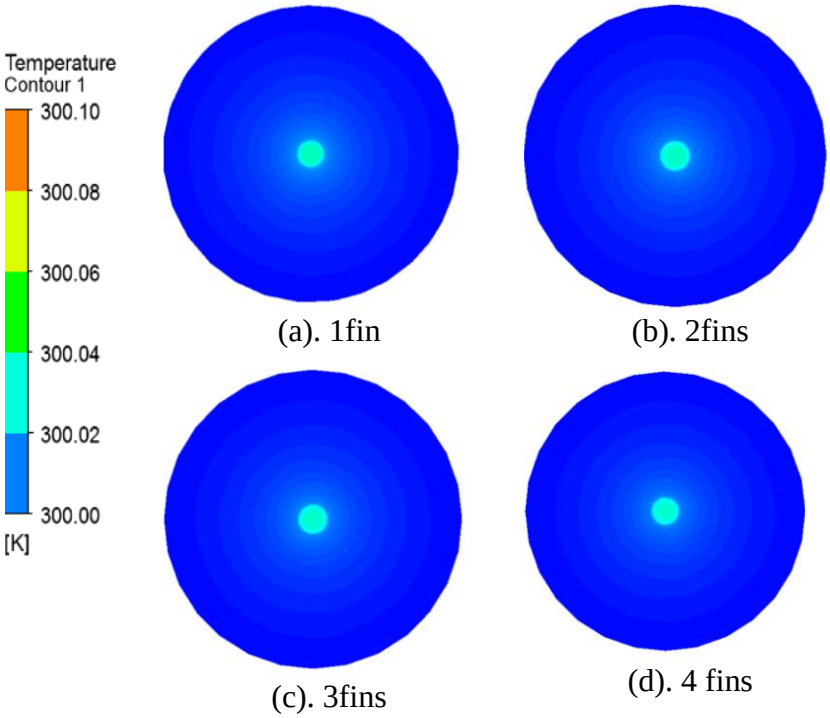


**Figure 24:** Outlet Temperatures cross section for soil conductivity 3.5 $Wm^{-1}K^{-1}$ and fin after every 0.5m (a). 1fin, (b). 2fins, (c). 3fins and (d). 4 fins

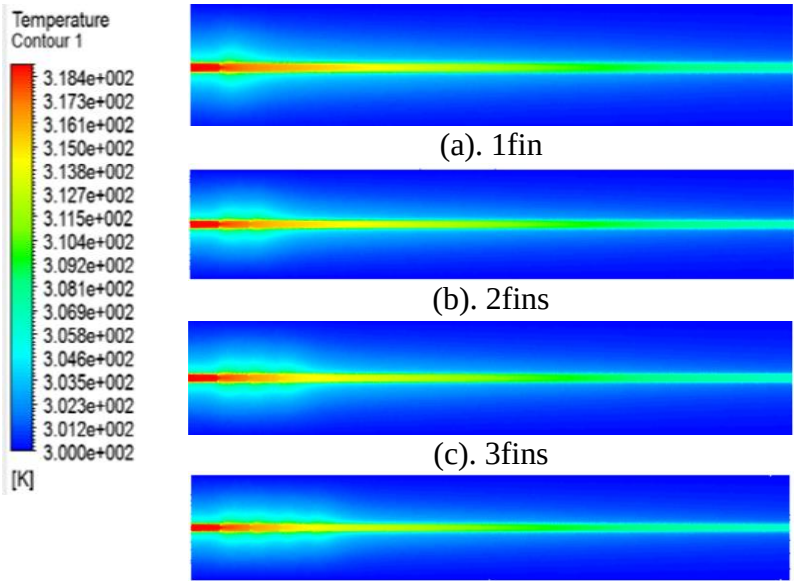


(a). 1fin

(b). 2fins

(c). 3fins

(d). 4fins

**Figure 25**: Heat dissipation in temperature contour on horizontal cross section area for fin after every 0.5 m (a). 1fin, (b). 2fins, (c). 3fins and (d). 4 fins.

Cross section along the length in the temperature contour gives a clear visual image in **Figure 24** and **Figure 25** for horizontal and outlet heat transfer taking place around the fins. Moreover, it is evident that the heat dissipation rate is more prominent near the fins than anywhere in the EATHE which helps to deteriorate the air temperature in the inlet to a lower temperature within a small time span. When the frequency of fins is changed to place them further away from each other, the temperature distribution is more even and steady over time.

### 5.3.2. 10 meter long after 1m distance

**Table 11**: Thermal effect of air temperature along the length with fins every 1m

| SL | No of fin | Position (m) | | | | | | | | | | |
|---|---|---|---|---|---|---|---|---|---|---|---|---|
| | | 0 | 1 | 2 | 3 | 4 | 5 | 6 | 7 | 8 | 9 | 10 |
| | | Temperature (K) | | | | | | | | | | |
| **1** | 1fin | 319 | 317.6 | 314.7 | 313.5 | 312.1 | 310.8 | 309.6 | 308.6 | 307.7 | 306.8 | 306.1 |
| **2** | 2fins | 319 | 317.4 | 314.5 | 313.3 | 311.9 | 310.6 | 309.4 | 308.4 | 307.5 | 306.6 | 305.9 |
| **3** | 3fins | 319 | 317.2 | 314.3 | 313.1 | 311.7 | 310.4 | 309.2 | 308.2 | 307.3 | 306.4 | 305.7 |
| **4** | 4fins | 319 | 317 | 314.1 | 312.9 | 311.5 | 310.2 | 309 | 308 | 307.1 | 306.2 | 305.5 |

**Table 11** displays the temperature at different lengths of the PVC when the EATHE is placed in the soil of thermal conductivity 3.5 $Wm^{-1}K^{-1}$ and the number of fin four. The expected result is obtained in the initial lengths, but the degradation slope deteriorates in the second half of the EATHE.

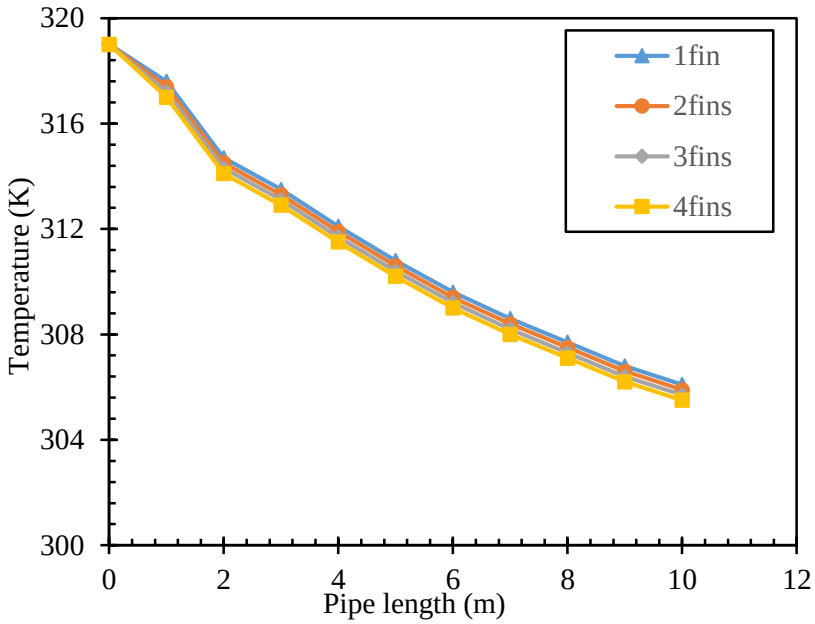


**Figure 26:** Temperature trend line along length for different fin every 1 m.

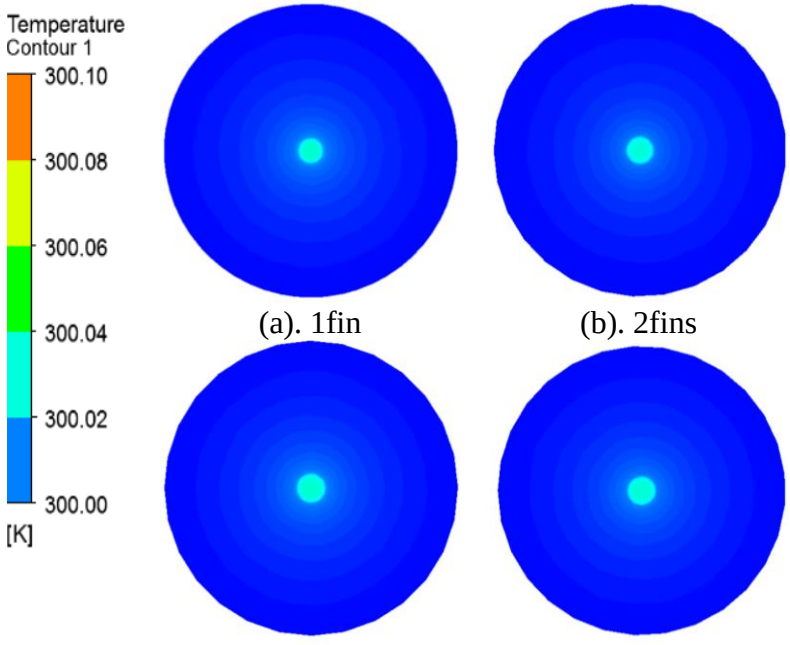


(a). 1fin (b). 2fins

(c). 3fins (d). 4 fins

**Figure 27:** Outlet Temperatures cross section for soil conductivity 3.5$Wm^{-1}K^{-1}$ and fin after every 1m (a). 1fin, (b). 2fins, (c). 3fins and (d). 4 fins.

The drop in temperature in the exit portion is negligible and doesn't vary to a noticeable extent when conductivity increases or pipe length increases. The rate of change of outlet temperature of the EATHE in the beginning length is higher than the exit portion of the length as the fins are placed only up to 4m in this arrangement. The slope of the outlet temperature curve where fins are present in **Figure 26** is steeper than the slope of length without fins. This result indicated the effect of multiple fins and increased heat transfer area to obtain low-temperature air in the lesser period. The graphical representation of the temperature contour in **Figure 27** and **Figure 28** is more practical with an increasing number of fins as it shows the heat transfer zone more visible than in the previous arrangement. The thermal gradient along the length of the cross-section is observed to spread air heat to the soil zone smoothly around the fins. Another observation is that the spreading of heat is less influenced by the adjacent fins when placed 1m apart than 0.5m apart. The first two fins dissipate more heat as the heat transfer is proportional to the temperature difference, and the soil zone is less influenced around the last two fins.

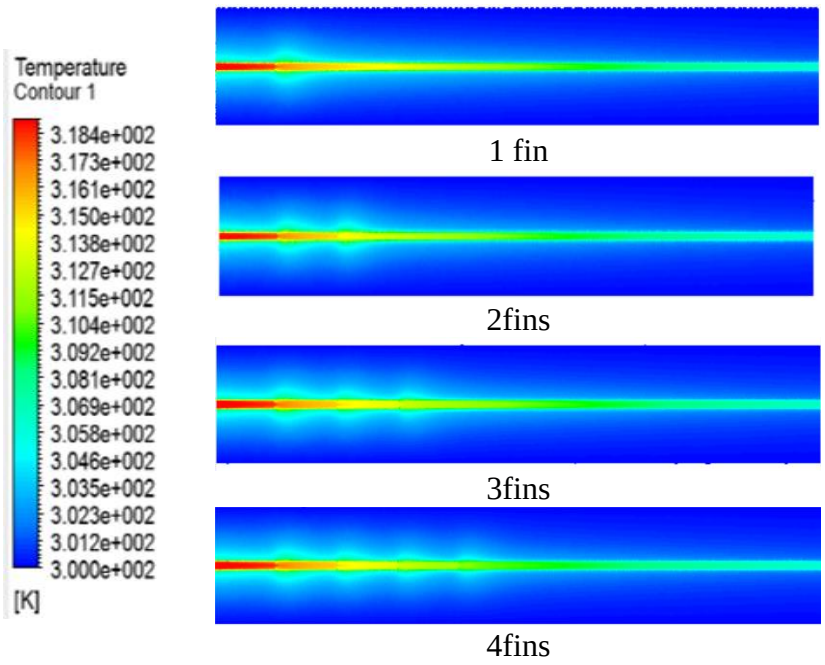


**Figure 28*:*** Heat dissipation in temperature contour on horizontal cross section area for fin after every 1m (a). 1fin, (b). 2fins, (c). 3fins and (d). 4 fins.

### 5.3.3. Ten meters long after two meter distance

**Table 12** is the instantaneous temperature of the numerical analysis of the arrangement where the inter-fin distance is 2m for the 10m EATHE with identical soil and air inlet velocity to the previous iterations. The specific length temperature of the two iterations is comparable where the performance degrades rather than improves. When fins are placed in this formation, the net number of fins that can be installed gets reduced, and the impact on the adjacent fin heat transfer degrades.

**Table 12**: Thermal effect of air temperature along the length with fins every 2 m.

| SL | No of fin | Position(m) | | | | | | | | | | |
|---|---|---|---|---|---|---|---|---|---|---|---|---|
| | | 0 | 1 | 2 | 3 | 4 | 5 | 6 | 7 | 8 | 9 | 10 |
| | | Temperature(K) | | | | | | | | | | |
| **1** | 1fin | 319 | 317.8 | 316 | 313.5 | 312.4 | 311.2 | 310.1 | 309.1 | 308.2 | 307.4 | 306.2 |
| **2** | 2fin | 319 | 317.5 | 315.7 | 313.2 | 312.1 | 310.9 | 309.8 | 308.8 | 307.9 | 307.1 | 305.9 |
| **3** | 3fin | 319 | 317.2 | 315.4 | 312.9 | 311.8 | 310.6 | 309.5 | 308.5 | 307.6 | 306.8 | 305.6 |
| **4** | 4fin | 319 | 316.9 | 315.1 | 312.6 | 311.5 | 310.3 | 309.2 | 308.2 | 307.3 | 306.5 | 305.3 |

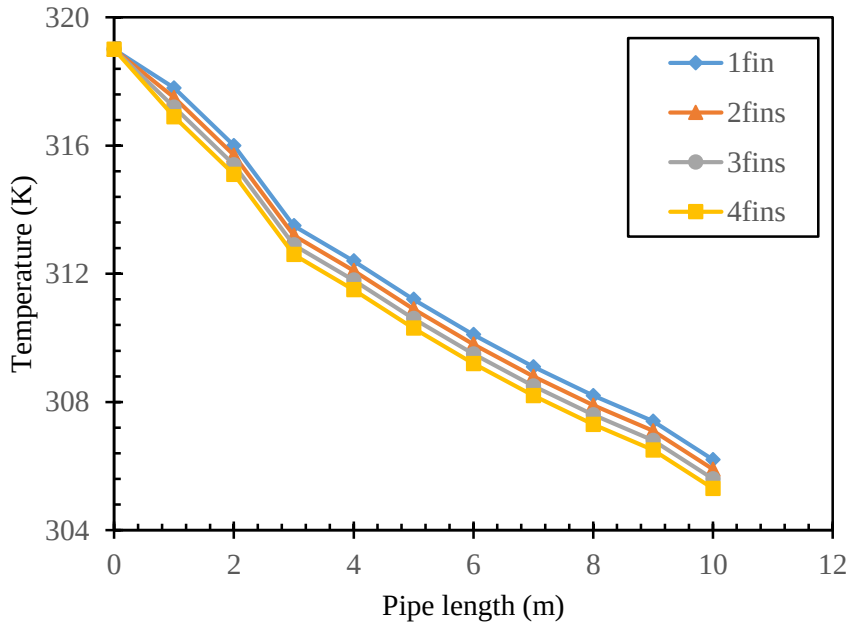


**Figure 29:** Temperature trend line along the length for different fin in every 2 m.

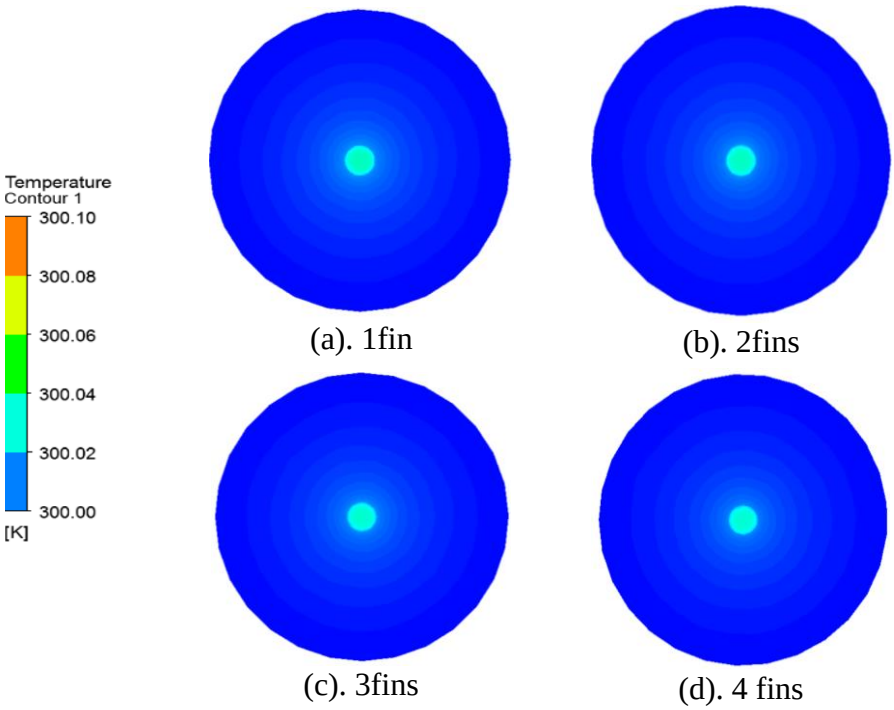


**Figure 30:** Outlet Temperatures cross section for soil conductivity 3.5$Wm^{-1}K^{-1}$ and fin after every 2 m (a). 1fin, (b). 2fins, (c). 3fins and (d). 4 fins.

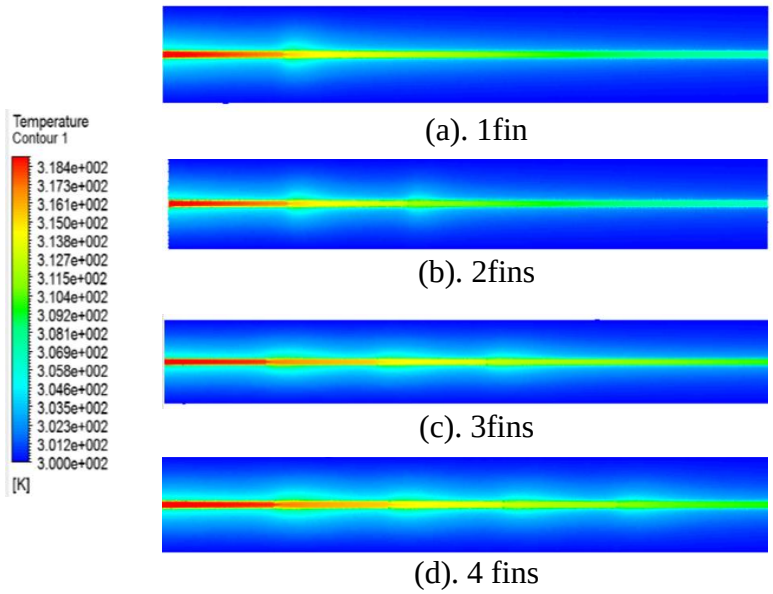


**Figure 31:** Heat dissipation in temperature contour on horizontal cross section area for fin after every 2 m (a). 1fin, (b). 2fins, (c). 3fins and (d). 4 fins.

**Figure 29** is the graphical representation of the temperature measured at every meter of the duct. The outlet temperature is found to be the lowest at 305.3K for four fins installed at 2m, 4m, 6m

and 8 m in length. The values obtained here have improved than that of 4 fins installed at 1 m inter-fin distance. The construction of the four fins remains the same, but their placement and spreading throughout the length help to transfer more heat from the air to the soil. The thermal gradient along the length in the cross-section in **Figure 30** and **Figure 31** spread air heat to the soil zone smoothly around the fins. Due to the heat transfer area of a fin compared to the pipe diameter, the influenced zone is most fruitful when the fins are placed 2 m.

The outlet temperature reduces by 1.48% that of the arrangement with fins separated by 1m and reduced by 6.2% of the temperature obtained by placing them 0.5m away from each other. Cross-section along the length shows a comparatively low thermally influenced zone around the fins than that of 1m inter fin distance. The drop in temperature evolves with four fins at 0.5 m, 1 m, 1.5 m and 2 m measured from the inlet. The graphical representation of the temperature profile with fins in place gives an identical trend line as the temperature drop with four fins in place is only 4.87% more than one fin in place.

### 5.4. Effect of number of fins on heat transfer performance

The effect of the number of fins installed on the thermal performance of the 10 m long pipe EATHE can be analyzed by comparing the data obtained for different arrangements in previous simulations. A uniform velocity 3 m/s and soil conductivity of 3.5 $Wm^{-1}K^{-1}$ are considered investigation for 10 m long pipe and a different numbers of the fin. When fins are placed in this formation, the net number of fins that can be installed gets reduced, and the impact on the adjacent fin heat transfer degrades.

#### 5.4.1. For Single Fin arrangement

**Table 13:** Thermal effect of air along the length with various fin spacing for a single fin

| Sl | No of fin 1 | Position(m) | | | | | | | | | | |
|---|---|---|---|---|---|---|---|---|---|---|---|---|
| | | 0 | 1 | 2 | 3 | 4 | 5 | 6 | 7 | 8 | 9 | 10 |
| | | Temperature(K) | | | | | | | | | | |
| **1** | After 0.5m | 319 | 316.5 | 315.3 | 314.5 | 312.6 | 311.3 | 310.2 | 309.1 | 308.2 | 307.4 | 306.7 |
| **2** | After 1m | 319 | 317.6 | 314.7 | 313.5 | 312.1 | 310.8 | 309.6 | 308.6 | 307.7 | 306.8 | 306.1 |
| **3** | After 2m | 319 | 317.8 | 316 | 313.5 | 312.4 | 311.2 | 310.1 | 309.1 | 308.2 | 307.4 | 306.2 |

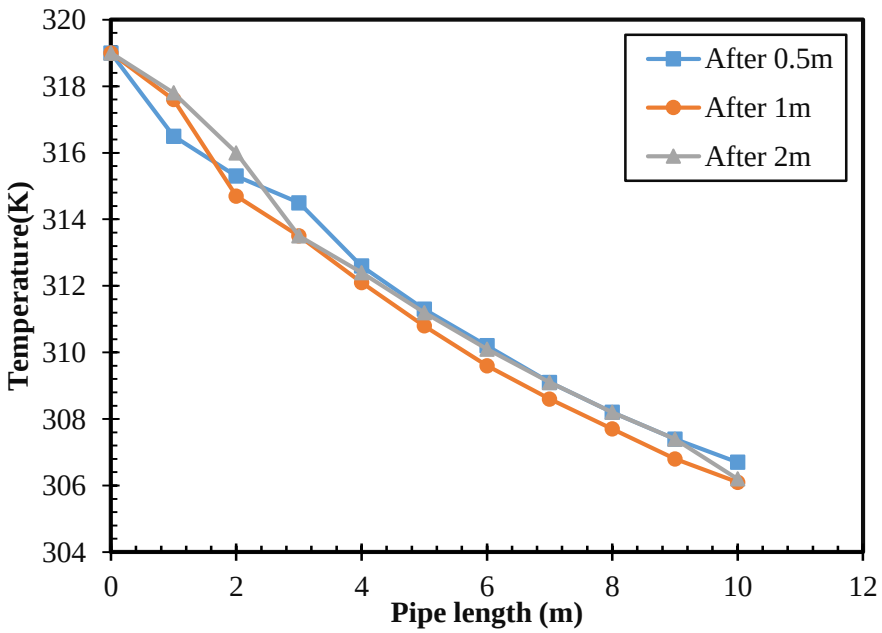


**Figure 32:** Temperature trend line of 10m pipe with one fin with different position

**Table 13** lists the air temperature at different lengths of the EATHE for a single fin installed at various locations in the initial portion of the duct. Graphical representation **Figure 32** of the temperatures for corresponding lengths indicate the position of the fin as the slope of the lines changes abruptly at the location of the installation. Better performance is obtained when the fins are separated by 1 m. The linear nature of the plot in the fin zone is proof of steady heat transfer. The maximum temperature drops at almost 12.9 K, which is 4.6% efficient from a fin placed 0.5 m apart from the inlet.

### 5.4.2. For double fins arrangement

**Table 14**: Thermal effect of air along the length with various fin spacing for two fins

| SL | No of fins 2 | Position (m) | | | | | | | | | | |
|---|---|---|---|---|---|---|---|---|---|---|---|---|
| | | 0 | 1 | 2 | 3 | 4 | 5 | 6 | 7 | 8 | 9 | 10 |
| | | Temperature (K) | | | | | | | | | | |
| **1** | After 0.5 m | 319 | 316.3 | 315.1 | 314.3 | 312.4 | 311.1 | 310 | 308.9 | 308 | 307.2 | 306.5 |
| **2** | After 1 m | 319 | 317.4 | 314.5 | 313.3 | 311.9 | 310.6 | 309.4 | 308.4 | 307.5 | 306.6 | 305.9 |
| **3** | After 2 m | 319 | 317.5 | 315.7 | 313.2 | 312.1 | 310.9 | 309.8 | 308.8 | 307.9 | 307.1 | 305.9 |

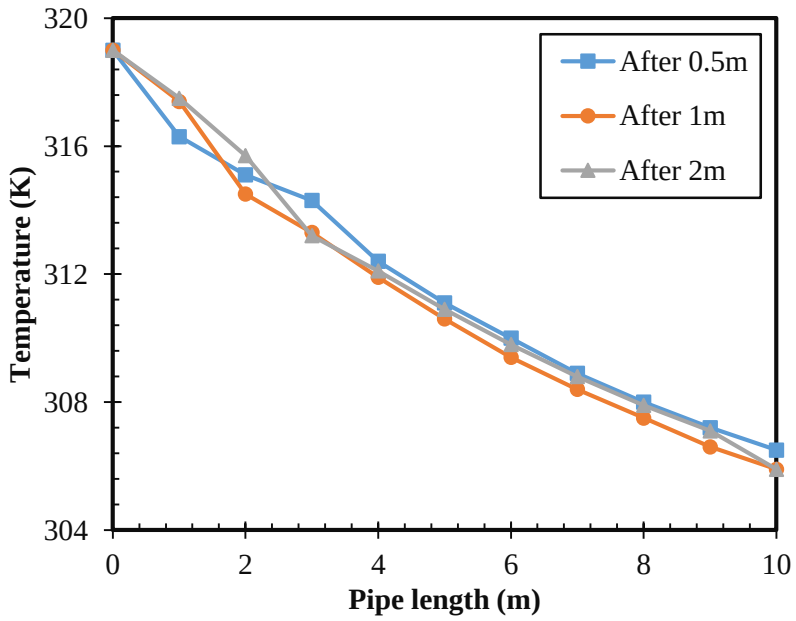


**Figure 33:** Temperature trend line of 10m pipe with two fins with different fin spacing.

Installation of 2 fins with different arrangements yields a similar performance pattern with improved results. **Table 14** shows the temperature profiles that change their value at specific locations where the fins are installed. Graphical representation **Figure 33** of the temperatures for corresponding lengths indicate the position of the fin as the slope of the lines changes abruptly on the location of the installation. The steeper slope represents the thermal performance improvement, and the linear segment shows the steady heat transfer that hampers the progress of the outlet air character. For the iteration with 2 m fin spacing, results improve by 2.34% as the outlet temperature is 306.2 K for the previous setup. Further development of the efficiency and performance occurs when more fins are installed due to the increased heat transfer area.

### 5.4.3. For three fins arrangement

The outlet temperature is reduced by 4.68% than for a single fin, but the efficiency changes are negligible. The deduction can be made on the results that the EATHE can be used to save more energy if they are accompanied by additional heat transfer areas or constrictions where the air can release heat to the soil around it. Table 15 shows thermal effect of air along the length with various fins, which gives the changes in heat transfer rate at different locations where fins are present.

**Table 15:** Thermal effect of air along the length with various fin spacing for three fins.

| SL | No of fins 3 | Position(m) | | | | | | | | | | |
|---|---|---|---|---|---|---|---|---|---|---|---|---|
| | | 0 | 1 | 2 | 3 | 4 | 5 | 6 | 7 | 8 | 9 | 10 |
| | | Temperature(k) | | | | | | | | | | |
| **1** | After 0.5m | 319 | 316.1 | 314.9 | 314.1 | 312.2 | 310.9 | 309.8 | 308.7 | 307.8 | 307 | 306.3 |
| **2** | After 1m | 319 | 317.2 | 314.3 | 313.1 | 311.7 | 310.4 | 309.2 | 308.2 | 307.3 | 306.4 | 305.7 |
| **3** | After 2m | 319 | 317.2 | 315.4 | 312.9 | 311.8 | 310.6 | 309.5 | 308.5 | 307.6 | 306.8 | 305.6 |

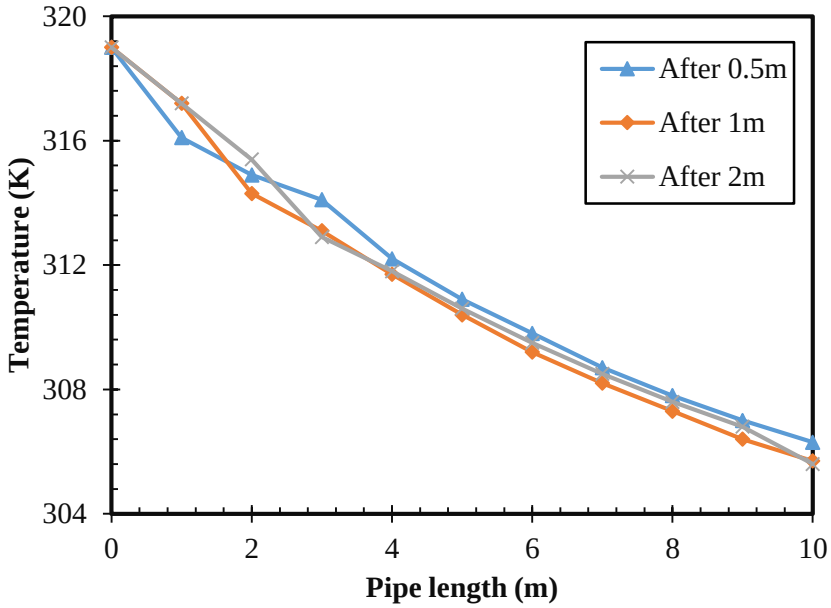


**Figure 34:** Temperature trend line of 10m pipe with three fins with different fin spacing

Three fins installed in various configurations produce similar performance patterns and better outcomes in temperature profiles whose values vary depending on where the fins are placed. The steeper slope shows the gain in thermal performance, and the consistent heat transfer led by the **Figure 34** linear segment prevents the outlet air quality from improving. For the iteration with 2m fin spacing, results improve by 1.2% as the outlet temperature is 305.6K for the previous setup. When more fins are placed, the efficiency and performance improve further due to the increased heat transfer area

### 5.4.4. For four fins arrangement

**Table 16:** Thermal effect of air along the length with various fin spacing for four fins.

| SL | No of fins 4 | Position(m) | | | | | | | | | | |
|---|---|---|---|---|---|---|---|---|---|---|---|---|
| | | 0 | 1 | 2 | 3 | 4 | 5 | 6 | 7 | 8 | 9 | 10 |
| | | Temperature(K) | | | | | | | | | | |
| **1** | After 0.5m | 319 | 315.9 | 314.7 | 313.9 | 312 | 310.7 | 309.6 | 308.5 | 307.6 | 306.8 | 306.1 |
| **2** | After 1m | 319 | 317 | 314.1 | 312.9 | 311.5 | 310.2 | 309 | 308 | 307.1 | 306.2 | 305.5 |
| **3** | After 2m | 319 | 316.9 | 315.1 | 312.6 | 311.5 | 310.3 | 309.2 | 308.2 | 307.3 | 306.5 | 305.3 |

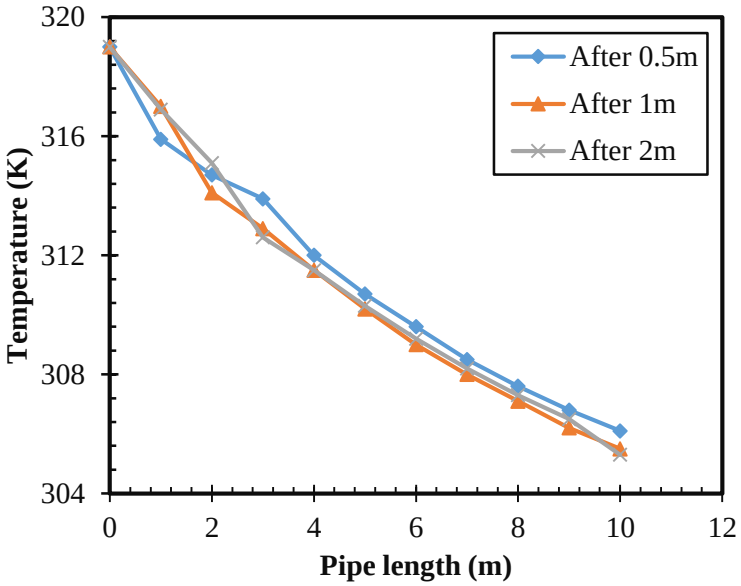


**Figure 35:** Temperature trend line of 10m pipe with four fins with different fin spacing

Outlet air temperature can be improved by increasing the number of fins, but the cost of installing the fins should be adequately considered. Moreover, the efficiency of the EATHE improves little with the further inclusion of fins. **Table 16** shows the measured temperatures of the air duct along the length. When the slope of the lines abruptly changes at the place of the installation, as seen in **Figure 35** of the corresponding lengths temperatures, the fin's position is shown. For example, the arrangement with four fins at 2 m spacing gives the outlet temperature of 305.3K, which is 7% better than a single fin. Still, the outlet air temperature for similar arrangements with three and four fins differs only by 0.3 K.

### 5.5. Effect of block introduction in the flow path

Replacing the fins of 10 mm thickness, a new arrangement of fins has been used to observe their effect on heat dissipation rate. In this arrangement, fins of 10 mm thickness and different heights have been used in diverging-converging patterns to restrict airflow and thus supply cooler air at the outlet. Each block consists of 5 fins of 15 mm, 20 mm, 25 mm, 20 mm, and 15 mm height placed equidistantly stretching to 2.5 m on the air to the boundary wall surface. The working fluid comes into contact with a larger fin area to dissipate more sensible heat in the blocks than in

the fins. When 1 block is implemented in the first quarter at the inlet of the EATHE, numerical data in **Table 17** shows that the heat transfer rate in this zone is higher than the rest of the length i.e., 2.17 K/m in the fin block and 0.84 K/m in the smooth portion. With 2 blocks in place, a similar trend is observed where the high heat transfer zone stretches up to the end of the blocks, which is at 5m from the inlet. The temperature drop profile in this region follows the trend line of 1 block up to 2.5 m and results in better performance to 5 m. **Figure 37** represents the outlet Temperatures profile of cross section for different block bodies in 10 m long pipe (a). 1 Block, (b). 2 Blocks, (c). 3 Blocks and (d). 4 Blocks.

**Table 17:** Temperature along the length with different numbers of blocks

| | Position | 1 Block | 2 Blocks | 3 Blocks | 4 Blocks |
|---|---|---|---|---|---|
| Temperature (K) | 0m | 319 | 319 | 319 | 319 |
| | 1m | 317.35 | 317.35 | 317.35 | 317.35 |
| | 2m | 314.52 | 314.52 | 314.52 | 314.05 |
| | 3m | 312.56 | 312.54 | 312.52 | 312.11 |
| | 4m | 311.64 | 310.62 | 310.6 | 310.31 |
| | 5m | 310.66 | 309.05 | 309.05 | 308.75 |
| | 6m | 309.54 | 308.15 | 307.85 | 307.55 |
| | 7m | 308.62 | 307.42 | 306.52 | 306.32 |
| | 8m | 307.83 | 306.74 | 305.72 | 305.45 |
| | 9m | 306.95 | 306.11 | 305.21 | 304.61 |
| | 10m | 305.76 | 304.98 | 304.36 | 303.84 |

With three blocks, a similar curve is obtained of '2 blocks' till 5m where the second block ends and gives high heat dissipation till 7.5m. The temperature drop profile imitates the '3 blocks' curve and continues the trend to the outlet of the pipe resulting in the best thermal performance. But in terms of efficiency, the result is not promising as the temperature drop does not multiply with the fin area getting multiplied in multiple blocks. Outlet temperature improves by 5.88% in the investigation with two blocks than in the '1 block' analysis. The value progresses to 10.53%

for three blocks and 14.52% for four blocks relative to the temperature drop of '1 block', which shows that the efficiency degrades with the increasing number of blocks but produces better thermal performance.

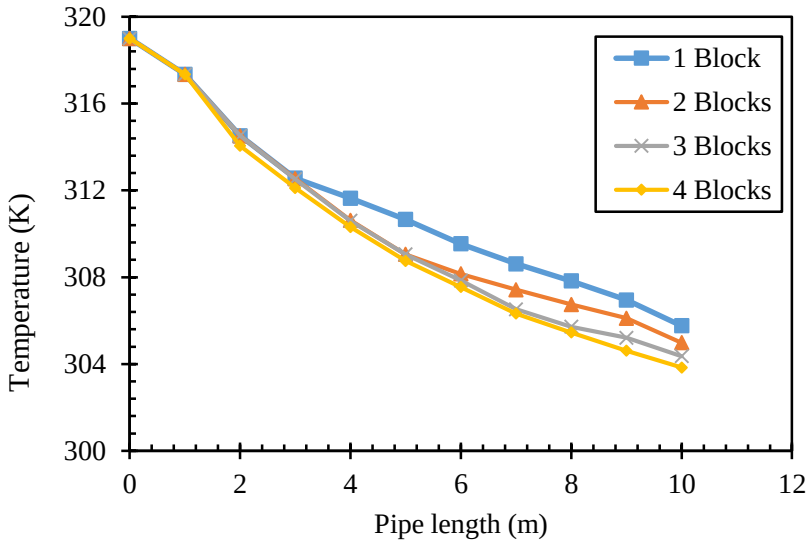


**Figure 36:** Temperature trend line of 10m pipe with blocks body.

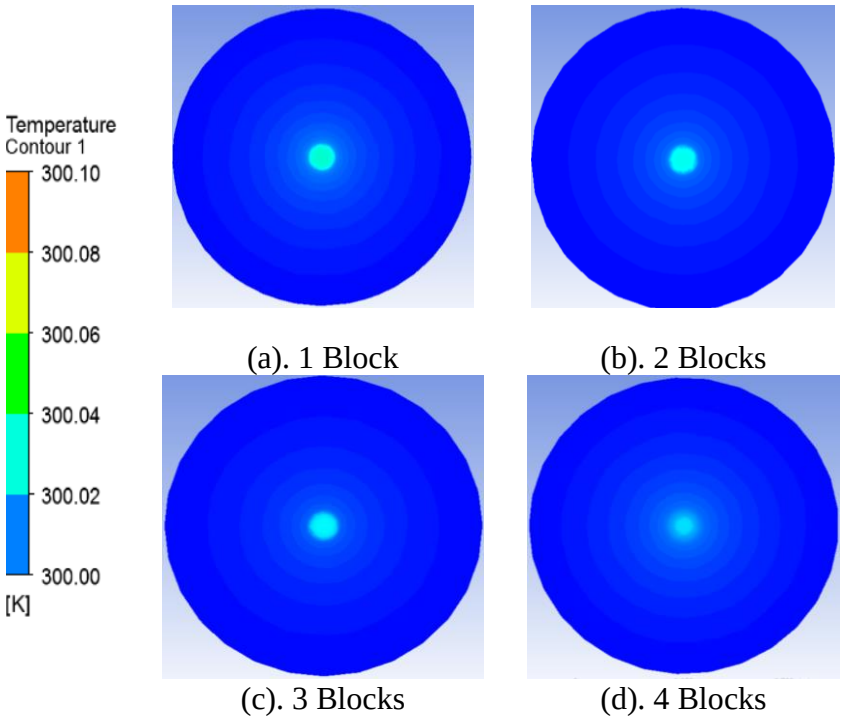


**Figure 37:** Outlet Temperatures cross section for different block bodies in 10 m long pipe (a). 1 Block, (b). 2 Blocks, (c). 3 Blocks and (d). 4 Blocks.

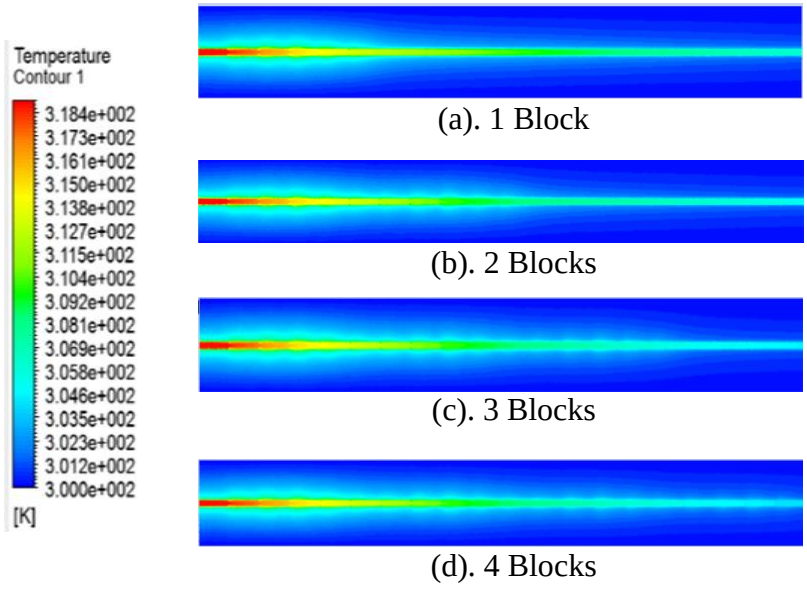


**Figure 38:** Heat dissipation in temperature contour on horizontal cross section area for (a). 1 Block, (b). 2 Blocks, (c). 3 Blocks and (d). 4 Blocks.

**Figure 38** is the visual representation of the temperature profile of heat spreading to the soil zone from air in the PVC duct, which can be used to understand the effect of the blocks in heat transfer from the system. The hot room air of 319 K is passed through the arrangement of the first block, where the extended area scatters the heat, affecting a larger soil zone than the rest of the length. The effect is more evident with four blocks which cover the entire length of the EATHE. The thermal gradient of the duct is visible to affect the surrounding soil zones throughout the blocks. The arrangement with four blocks yields the best thermal performance of the 4 cases taken into consideration to analyze the improvement parameters of an EATHE.

# 6. Chapter: Conclusion and Future Scope

## 6.1. Summary

This study investigates the influence of soil thermal conductivity, air velocity, PVC pipe thickness, and length on the EATHE model. The thermal performance based on three miscellaneous soil samples, each having a different thermal conductivity, is 0.65 $Wm^{-1}K^{-1}$, 1.25 $Wm^{-1}K^{-1,}$ and 3.5 $Wm^{-1}K^{-1}$.

The following are the key findings of this study:

- The effect of the soil layer is negligible after a critical thickness. The critical thickness considers ten times on pipe diameter.
- The best result is obtained with the highest thermal conductivity and lowest inlet air velocity because of the proportional relation of air particle to pipe wall interaction time and heat transfer rate. For example, in case study 1, the maximum temperature declines 18.9 K for 3.5 $Wm^{-1}K^{-1}$ thermal conductivity at a specific air velocity of 3 $ms^{-1}$.
- The effect of fins was analyzed by placing a single fin of 10mm at 0.5m from the inlet and getting an outlet temperature of 306.7 K. The drop in temperature evolves with four fins, 0.5 m, 1m, 1.5 m, and 2 m, and get minimum temperature is 306.1 K which is 19.4% more performed from the straight pipe. If fins are placed every one meter apart, the temperature drop increases 5.6% more.
- The arrangement with four fins at 2 m spacing gives the outlet temperature of 305.3 K, which is 7% better than a single fin.
- The result is not promising as the temperature drop does not multiply with the fin area getting multiplied in multiple blocks. However, outlet temperature improves by 5.88% in the investigation with two blocks than in the ‘1 block’ analysis. The value progresses to 10.53% for three blocks and 14.52% for four blocks relative to the temperature drop of ‘one block’, which

shows that the efficiency degrades with an increasing number of blocks but produces better thermal performance.

### 6.2. Scopes for future work

- In this study, a straight PVC pipe is used as the flow passage for the fluid for the heat exchanger. The effect of heat transfer and friction properties on laminar and turbulent flow under transient conditions is examined. Furthermore, this straight PVC pipe can be exchanged for a rectangular or curved PVC pipe because it impacts the flow area. As a result, it can be regarded for further research from the standpoint of interest.
- The Reynolds Stress Turbulence Model or another comparable model can be used to investigate the turbulent flow range numerically.
- The ring fin explored in this work can be substituted by a sinusoidal type fin to demonstrate the effects of heat transfer and pressure drop performance,

# 7. Chapter: References

References


1. Xamán, J., et al., *Numerical study of earth-to-air heat exchanger: The effect of thermal insulation.* Energy and buildings, 2014. **85**: p. 356-361.
2. Pérez-Lombard, L., J. Ortiz, and C. Pout, *A review on buildings energy consumption information.* Energy and buildings, 2008. **40**(3): p. 394-398.
3. Jacovides, C., et al., *On the ground temperature profile for passive cooling applications in buildings.* Solar energy, 1996. **57**(3): p. 167-175.
4. Nejat, P., et al., *A global review of energy consumption, CO2 emissions and policy in the residential sector (with an overview of the top ten CO2 emitting countries).* Renewable and sustainable energy reviews, 2015. **43**: p. 843-862.
5. Mihalakakou, G., M. Santamouris, and D. Asimakopoulos, *Modelling the thermal performance of earth-to-air heat exchangers.* Solar Energy (Journal of Solar Energy Science and Engineering);(United States), 1994. **53**(3).
6. Sawhney, R., D. Buddhi, and N. Thanu, *An experimental study of summer performance of a recirculation type underground airpipe air conditioning system.* Building and Environment, 1998. **34**(2): p. 189-196.
7. Vaz, J., et al., *Experimental and numerical analysis of an earth–air heat exchanger.* Energy and Buildings, 2011. **43**(9): p. 2476-2482.
8. Jayashankar, B., R. Sawhney, and M. Sodha, *Effect of different surface treatments of the surrounding earth on thermal performance of earth-integrated buildings.* International Journal of Energy Research, 1989. **13**(5): p. 605-619.
9. Givoni, B. and L. Katz, *Earth temperatures and underground buildings.* Energy and Buildings, 1985. **8**(1): p. 15-25.
10. Omer, A.M., *Ground-source heat pumps systems and applications.* Renewable and sustainable energy reviews, 2008. **12**(2): p. 344-371.
11. Esen, H., M. Inalli, and M. Esen, *Numerical and experimental analysis of a horizontal ground-coupled heat pump system.* Building and environment, 2007. **42**(3): p. 1126-1134.
12. Bharadwaj, S. and N. Bansal, *Temperature distribution inside ground for various surface conditions.* Building and Environment, 1981. **16**(3): p. 183-192.
13. Deshmukh, M., M. Sodha, and R. Sawhney, *Effect of depth of sinking on thermal performance of partially underground building.* International Journal of Energy Research, 1991. **15**(5): p. 391-403.
14. Esen, H., M. Esen, and O. Ozsolak, *Modelling and experimental performance analysis of solar-assisted ground source heat pump system.* Journal of Experimental & Theoretical Artificial Intelligence, 2017. **29**(1): p. 1-17.
15. Lucia, U., et al., *Ground-source pump system for heating and cooling: Review and thermodynamic approach.* Renewable and Sustainable Energy Reviews, 2017. **70**: p. 867-874.
16. İnallı, M. and H. Esen, *Experimental thermal performance evaluation of a horizontal ground-source heat pump system.* Applied thermal engineering, 2004. **24**(14-15): p. 2219-2232.
17. Wu, W., et al., *Simulation of a combined heating, cooling and domestic hot water system based on ground source absorption heat pump.* Applied energy, 2014. **126**: p. 113-122.
18. Balbay, A. and M. Esen, *Experimental investigation of using ground source heat pump system for snow melting on pavements and bridge decks.* Scientific Research and Essays, 2010. **5**(24): p. 3955-3966.
19. Balbay, A. and M. Esen, *Temperature distributions in pavement and bridge slabs heated by using vertical ground-source heat pump systems.* Acta Scientiarum. Technology, 2013. **35**(4): p. 677-685.

20. Esen, H., M. Inalli, and M. Esen, *A techno-economic comparison of ground-coupled and air-coupled heat pump system for space cooling.* Building and environment, 2007. **42**(5): p. 1955-1965.
21. Khatry, A., M. Sodha, and M. Malik, *Periodic variation of ground temperature with depth.* Solar Energy, 1978. **20**(5): p. 425-427.
22. Wu, H., S. Wang, and D. Zhu, *Modelling and evaluation of cooling capacity of earth–air–pipe systems.* Energy Conversion and Management, 2007. **48**(5): p. 1462-1471.
23. Bansal, N., M. Sodha, and S. Bharadwaj, *Performance of earth air tunnels.* International Journal of Energy Research, 1983. **7**(4): p. 333-345.
24. Santamouris, M., A. Argiriou, and M. Vallindras, *Design and operation of a low energy consumption passive solar agricultural greenhouse.* Solar energy, 1994. **52**(5): p. 371-378.
25. Ozgener, L., *A review on the experimental and analytical analysis of earth to air heat exchanger (EAHE) systems in Turkey.* Renewable and Sustainable Energy Reviews, 2011. **15**(9): p. 4483-4490.
26. Bisoniya, T.S., A. Kumar, and P. Baredar, *Experimental and analytical studies of earth–air heat exchanger (EAHE) systems in India: a review*. Renewable and Sustainable Energy Reviews, 2013. **19**: p. 238-246.
27. Peretti, C., et al., *The design and environmental evaluation of earth-to-air heat exchangers (EAHE). A literature review*. Renewable and Sustainable Energy Reviews, 2013. **28**: p. 107-116.
28. Kaushal, M., *Geothermal cooling/heating using ground heat exchanger for various experimental and analytical studies: Comprehensive review.* Energy and Buildings, 2017. **139**: p. 634-652.
29. Kumar, R., S. Kaushik, and S. Garg, *Heating and cooling potential of an earth-to-air heat exchanger using artificial neural network.* Renewable Energy, 2006. **31**(8): p. 1139-1155.
30. Puri, V., *Heat and mass transfer analysis and modeling in unsaturated ground soils for buried tube systems.* Energy in Agriculture, 1987. **6**(3): p. 179-193.
31. Bojić, M., G. Papadakis, and S. Kyritsis, *Energy from a two-pipe, earth-to-air heat exchanger.* Energy, 1999. **24**(6): p. 519-523.
32. Krarti, M. and J.F. Kreider, *Analytical model for heat transfer in an underground air tunnel.* Energy conversion and management, 1996. **37**(10): p. 1561-1574.
33. Deglin, D., L. Van Caenegem, and P. Dehon, *Subsoil heat exchangers for the air conditioning of livestock buildings.* Journal of agricultural engineering research, 1999. **73**(2): p. 179-188.
34. Thiers, S. and B. Peuportier, *Thermal and environmental assessment of a passive building equipped with an earth-to-air heat exchanger in France.* Solar Energy, 2008. **82**(9): p. 820-831.
35. Bansal, V., et al., *Performance analysis of earth–pipe–air heat exchanger for winter heating.* Energy and Buildings, 2009. **41**(11): p. 1151-1154.
36. Bansal, V., et al., *Performance analysis of earth–pipe–air heat exchanger for summer cooling.* Energy and Buildings, 2010. **42**(5): p. 645-648.
37. Bansal, V., et al., *'Derating Factor'new concept for evaluating thermal performance of earth air tunnel heat exchanger: A transient CFD analysis.* Applied Energy, 2013. **102**: p. 418-426.
38. Bansal, V., et al., *Transient effect of soil thermal conductivity and duration of operation on performance of Earth Air Tunnel Heat Exchanger.* Applied Energy, 2013. **103**: p. 1-11.
39. Ozgener, O., L. Ozgener, and A. Yildiz, *Designing of a photovoltaic assisted earth to air heat exchanger*. 2010, Project.
40. Misra, R., et al., *Transient analysis based determination of derating factor for Earth Air Tunnel Heat Exchanger in winter.* Energy and Buildings, 2013. **58**: p. 76-85.
41. Misra, R., et al., *Transient analysis based determination of derating factor for earth air tunnel heat exchanger in summer.* Energy and buildings, 2013. **58**: p. 103-110.
42. Misra, R., et al., *CFD analysis based parametric study of derating factor for Earth Air Tunnel Heat Exchanger.* Applied Energy, 2013. **103**: p. 266-277.

43. Li, H., et al., *Performance of a coupled cooling system with earth-to-air heat exchanger and solar chimney.* Renewable Energy, 2014. **62**: p. 468-477.
44. Mathur, A., et al., *Transient effect of soil thermal diffusivity on performance of EATHE system.* Energy Reports, 2015. **1**: p. 17-21.
45. Mathur, A., et al., *Comparative study of straight and spiral earth air tunnel heat exchanger system operated in cooling and heating modes.* Renewable Energy, 2017. **108**: p. 474-487.
46. Misra, R., T.K. Aseri, and V. Bansal. *CFD analysis of thermal influence zone of earth air tunnel heat exchanger under transient conditions*. in *Proceedings of BS2015 14th Conference of International Building Performance Simulation Association, Hyderabad, India*. 2015.
47. de Jesus Freire, A., et al., *Compact buried pipes system analysis for indoor air conditioning.* Applied Thermal Engineering, 2013. **51**(1-2): p. 1124-1134.
48. Kabashnikov, V., et al., *Analytical and numerical investigation of the characteristics of a soil heat exchanger for ventilation systems.* International Journal of Heat and Mass Transfer, 2002. **45**(11): p. 2407-2418.
49. Sodha, M., U. Mahajan, and R. Sawhney, *Thermal performance of a parallel earth air-pipes system.* International Journal of Energy Research, 1994. **18**(4): p. 437-447.
50. Mathur, A., et al., *Investigation of soil thermal saturation and recovery under intermittent and continuous operation of EATHE.* Energy and Buildings, 2015. **109**: p. 291-303.
51. Mathur, A., A.K. Surana, and S. Mathur, *Numerical investigation of the performance and soil temperature recovery of an EATHE system under intermittent operations.* Renewable energy, 2016. **95**: p. 510-521.
52. Mathur, A., et al., *CFD analysis of EATHE system under transient conditions for intermittent operation.* Energy and Buildings, 2015. **87**: p. 37-44.
53. Al-Ajmi, F., D. Loveday, and V.I. Hanby, *The cooling potential of earth–air heat exchangers for domestic buildings in a desert climate.* Building and Environment, 2006. **41**(3): p. 235-244.
54. Goswami, D. and A. Dhaliwal, *Heat transfer analysis in environmental control using an underground air tunnel.* 1985.